A STUDY TO IMPROVE THE LIFE OF HIGH SPEED STEEL TOOLS WITH ION PLATED REFRACTORY COMPOUNDS

A THESIS

Presented to

The Faculty of the Division

of Graduate Studies

By

Potru China Subbarao

In Partial Fulfillment

of the Requirements for the Degree

Doctor of Philosophy

in the School of Mechanical Engineering

Georgia Institute of Technology

October, 1979

A STUDY TO IMPROVE THE LIFE OF HIGH SPEED STEEL TOOLS WITH ION PLATED REFRACTORY COMPOUNDS

APPROVED:

Carl H. Jacobs, Chairman

John T. Berry

Stuart J. Deutsch

Stephen Spooner

Date approved by Chairman: 10/12/79

ACKNOWLEDGMENTS

The author would like to take this opportunity to thank all the individuals who have contributed to the completion of this dissertation. In particular he wishes to thank Dr. C. H. Jacobs, his thesis advisor, for his advice and encouragement during the course of this work. The author is deeply grateful to Dr. John T. Berry for his editorial comments and interest in this research. The critical comments given by Dr. S. Ramalingam have been helpful and they are duly acknowledged. Dr. S. Spooner has been very helpful in the performance of critical experiments on texture and diffraction. The author would also like to thank Dr. S. J. Deutsch for his valuable suggestions and comments in the planning stage of this investigation.

This work was sponsored by Southern Saw Corporation (under Grant E25-675) whose support is deeply appreciated. At the same time, the author thanks Mr. Thomas D. Harris of Southern Saw Corporation for his excellent cooperation and help.

Particular thanks should be conveyed to Dr. S. Peter Kezios, Director of the School of Mechanical Engineering, for provision of the research facilities. The author wishes to thank Mr. Harry Vaughan of the Mechanical Engineering machining and toolroom facility for special

assistance, Mr. Y. B. Rao for help in chemical analysis, Dr. K. Sudarsanan for assistance in X-ray diffraction and Mr. Ronnie W. Camp, of Micromeritics Instrument Corporation, for his patience and encouragement.

Last but not the least, the author would like to express his appreciation to his wife, Parvati Devi, for her understanding and love during the entire period of this project. The author likes to take this moment to say 'thank you' to his mother, Potru Tulasamma for her untiring sacrifice and encouragement during the entire education of the author.

TABLE OF CONTENTS

Page

ACKNOWLEDGMENTS. ii

LIST OF TABLES vi

LIST OF ILLUSTRATIONS. vii

SUMMARY. ix

Chapter

I. INTRODUCTION 1

II. LITERATURE REVIEW. 6

Metal Cutting Tools
Coating Technology

III. EXPERIMENTAL PROGRAM TECHNIQUES AND PROCEDURES . . 31

Ion Plating System
Preparation of the Tools
Characterization of the Coated Tools
Tool Life Testing of the Coated Tools

IV. RESULTS. 45

Surface Observation of the Tools
Characterization of the Coating
Stoichiometry of the Coating
Texture of the Coating
Characteristics of the Coating Cross Section
Work Material Characterization
Evaluation of the Tool Wear

V. DISCUSSION OF RESULTS. 79

Preparation of the Coating
Post Heat Treatment of the Tools
Chemistry and Structure of the Coating
Preferred Orientation of the Coating
Performance of the Tools

VI. CONCLUSIONS AND RECOMMENDATIONS. 93

Appendix Page

A. STOICHIOMETRY OF TITANIUM CARBIDE COATING. 98

B. POWDER DIFFRACTION PATTERN OF AS-COATED AISI M-1 TOOL. 99

C. CALCULATION OF LATTICE PARAMETER OF COATED TiC . . 101

D. MAGNETIC FIELD STRENGTH OF DC COIL 105

E. QUANTITATIVE AES ANALYSIS. 107

F. CALCULATION OF AMOUNTS OF TITANIUM AND CARBON IN THE COATING 110

G. USE OF EPMA FOR THIN FILM CHARACTERIZATION 112

H. TOOL-CHIP FRICTION COEFFICIENT CALCULATION 113

I. SUBSTRATE-COATING INTERFACE HARDNESS 115

BIBLIOGRAPHY. 118

VITA. 128

LIST OF TABLES

Table		Page
1.	Cutting Conditions for Tool Life Experiments. . .	44
2.	Auger Electron Spectroscope (AES) Data for the Coating	56
3.	Chemical Analysis of AISI 1045.	60
4.	Flank Wear Data	62
5.	Flank Wear Data	63
6.	Flank Wear Data	64
7.	Flank Wear Data	65
8.	Crater Depth Measurements for Uncoated, 2 μm Thick Coated and 4 μm Thick Coated AISI M-1 Tools at Cutting Conditions 175 ft/min, 0.0075 in/rev and 0.060 in.	67
9.	Flank Wear Data	70
10.	Flank Wear Data	71
11.	Flank Wear Data	72
12.	Flank Wear Data	74
13.	Flank Wear Data	75
14.	Flank Wear Data	77
C-1.	Lattice Parameter of the Coating.	103
E-1.	Atomic Concentration in the Coating	109
H-1.	Cutting Force and Friction Coefficient Data . . .	114

LIST OF ILLUSTRATIONS

Figure		Page
1.	Tool Insert.	8
2.	Discharge Tube	21
3.	Ductile-Brittle Transition in Carbides	34
4.	Schematic Diagram of Ion Plating System.	37
5.	2^3+ Center Point Design Used for Tool Life Experiment	43
6.	Scanning Electron Micrograph of Surface Topography of AISI M-1 Tool.	46
7.	Scanning Electron Micrograph of AISI M-1 Tool Electropolished and Etched	47
8.	Scanning Electron Micrograph of Isometric View of Ion Plated and Heat Treated AISI M-1 Tool	49
9.	Scanning Electron Micrograph of Surface Topography of Ion Plated and Heat Treated AISI M-1 Tool.	50
10.	Powder Diffraction (X-Ray) Pattern of Coated and Heat Treated AISI M-1 Tool	51
11.	TiC Coating Texture Pole (111)	53
12.	TiC Coating Texture Pole (200)	54
13.	Sputtering Time Vs. Elements in the Coating. . .	55
14.	Scanning Electron Micrographs of Ion Plated, Heat Treated and Fractured AISI M-1 Tool	57
15.	Scanning Electron Photomicrograph of Ion Plated, Heat Treated, Polished and 10% Nital Etched Section of AISI M-1 Tool.	58
16.	Hardness Profile Along the Radius from the Center of Work Material.	61

Figure		Page
17.	Wear Land Width Vs. Cutting Time at 175 ft/min Cutting Speed, 0.0075 in/rev Feed and 0.060 in Depth of Cut.	66
18.	Scanning Electron Micrographs of Uncoated and Coated (4 μm) AISI M-1 Tools after 15 Minutes of Turning at 175 ft/min, 0.0075 in/rev and 0.060 in	68
19.	Wear Land Width Vs. Cutting Time at 175 ft/min Cutting Speed, 0.0025 in/rev Feed and 0.060 in Depth of Cut	73
20.	Wear Land Width Vs. Cutting Time at 125 ft/min Cutting Speed, 0.0025 in/rev Feed and 0.060 in Depth of Cut	76
21.	Wear Land Width Vs. Cutting Time at 150 ft/min, Cutting Speed, 0.005 in/rev Feed and 0.060 in Depth of Cut	78
B-1.	Powder Diffraction (X-Ray) Pattern of As-Coated AISI M-1 Tool.	100
C-1.	Extrapolation Curve for Lattice Parameter of TiC Coating.	104
I-1.	Micro-Hardness Vs. Coating Depth	116
I-2.	Photomicrograph of Taper Section with Indentations	117

SUMMARY

A classical metal cutting process involves a work material, a tool material (tool) and relative motion between the two. A significant portion of the energy put into the cutting process is expended as heat in a small volume of material. This local temperature rise at the cutting edge can lead to localized softening of the tool. This in turn may result in one or more types of tool wear and hence reduced tool life. As the heating process is inherent in machining, cutting tool life should be independent of temperature and can be improved either by working with the bulk of the tool to negate the local heating effects or by improving the wear resistance of the surface of the tool.

The wear resistance of the surface may be enhanced by surface heat treatment and/or by depositing a wear resistant layer on the surface of the tool. The objective of this research was to investigate the effect of a titanium carbide type coating, obtained by ion plating and post heat treatment, on the life of a high speed steel turning tool.

Prehardened and ground high speed steel (AISI M-1) tools were ion plated with titanium. The tools were then heat treated in vacuo and quenched in argon to convert the titanium to titanium carbide. The titanium carbide thus obtained was identified by X-ray diffraction technique and

the chemical composition of the coating was established with an Electron Probe Microanalyzer (EPMA). Auger Electron Spectroscopy (AES) was used to evaluate the coating composition variation with coating depth. A fracture cross section of the coated tool was studied in the Scanning Electron Microscope (SEM) to evaluate the adhesion of the coating to the substrate. Tool life experiments were then designed and conducted in order to evaluate the performance of the coated and uncoated tools against tool wear.

Ion plating as used in this study requires post heat treatment of the tool to convert the ion plated titanium to titanium carbide. The composition of the coating formed was confirmed to be titanium carbide with a variable stoichiometry across the rake face of the tool insert. The titanium carbide coating has a preferred orientation with the cube faces developing from the (0001) basal planes of the as-deposited close packed hexagonal titanium.

Flank wear tests were conducted by turning hot rolled, fine grain, silicon killed, special quality AISI 1045 steel with coated as well as uncoated tools. These tests demonstrate that the coated tools have superior life when compared with uncoated tools. That is the titanium carbide thin films, as studied here, decrease the wear rate of AISI M-1 tool substrate for all test conditions evaluated. Crater wear measurements also support this finding. The reasons for this superior performance are thought to be good

stoichiometry of titanium carbide and good adhesion of the coating to the substrate.

CHAPTER I

INTRODUCTION

Manufacturing is an interaction between mankind, machines and materials. Of all the materials used in manufacturing, metals still occupy a prominent place. Unless the product is used in the as-cast condition or brought to final shape by either forming or by powder metallurgy techniques, machining of metals and alloys plays an important role in bringing the product to final dimensions. Machining as defined here involves a cutting tool, work material and relative motion between the two. Consequently, the cutting tool is an important part of the machining system.

At the turn of the nineteenth century, metal cutting tools were produced from unalloyed high carbon steel.[1] This material can take a very keen cutting edge and is still used in the manufacture of hand tools, razor blades, meat cutting saw blades and wood cutting tools. However, the temperature of the cutting edge must be held below 200 C (392 F) if the tool is to retain its cutting edge, as the hardness of the high carbon steel falls off above this temperature due to tempering. The tempering effect of high temperatures is a critical parameter in the design of any cutting tool material. This effect is particularly important when one considers the

fact that in order to increase production rates in a given manufacturing process cutting speed must be increased. The increase in speed increases the local tool temperature thereby weakening it even faster.

In the early 1900's F. W. Taylor and associated metallurgists developed the 18-4-1 (18% tungsten, 4% chromium, 1% vanadium, 0.8% carbon, balance iron) high speed steel (HSS), now standardized as AISI T-1 and essentially revolutionized the whole metal cutting industry. Cutting tools made of this material retain their cutting edge to temperatures of about 500 C (932 F). The speeds at which metal could be removed were more than doubled in comparison with plain high carbon steel, with a resulting increase in production rates. Subsequently, many HSS alloys have been developed to increase the tempering temperature of the resultant tool so that increased cutting speeds could be utilized. Current high speed steel alloys[4] are essentially high carbon steels containing about 4% chromium, 1-5% vanadium, varying amounts of both tungsten and molybdenum and often varying amounts of cobalt. High speed steel is composed of a considerable quantity of hard complex primary, alloy carbides embedded in a matrix containing both carbon in solid solution or as temper or secondary carbides and a portion of the alloying elements that are present again either in secondary carbides or in solid solution. In the annealed condition, the steels have a ferrite matrix with a

large volume fraction of undissolved carbides present. In the as-hardened condition they contain martensite, retained austenite and undissolved carbides. The amount of retained austenite must be minimized to achieve proper hardness. The martensite matrix possesses very reasonable measures of toughness and strength over a wide range of temperature and supports a dispersion of hard wear-resistant carbides. After tempering, which may often be of a multiple variety, the structure contains tempered martensite (which is essentially a fine grained product containing finely dispersed second phases or zones), undissolved carbides and little or no retained austenite.

More recently cemented carbides and ceramics have been introduced as cutting tool materials. Each tool alloy development helped to supplement the older materials. Cemented carbides are mixtures of tungsten carbide (WC), titanium carbide (TiC) and tantalum carbide (TaC), with the binding material being predominantly cobalt (Co)[2]. Increasing the cobalt content reduces the brittleness and increases the strength of the tool. It also reduces the hot-hardness and gives lower resistance to thermal deformation and cratering. The addition of titanium carbide will increase the wear and cratering resistance; the hot-hardness and resistance to thermal deformation will be improved, but there will be a decrease of strength and thermal conductivity and increase in brittleness. Tantalum carbide improves the hot-hardness

of cemented carbides and therefore the resistance to thermal deformation is even better than with titanium carbide additions, but it is less effective in cratering resistance and it reduces wear resistance and strength.

A very recent advance in cutting tool technology has been the introduction of the coated carbide tool by Sandvik in 1969.[3] Some twenty percent of the cutting tools sold today are coated carbides; within the next three to five years, the percentage may reach sixty. It is well known that titanium carbide shows a high resistance against cratering and wear because it creates less friction between the chip and the tool rake face.[2] The titanium carbide coated cemented carbide, makes use of normal available strength and provides a skin of crater resistant material, thus being able to solve a lot of cutting tool problems. Hence, the growing application of coated cemented tungsten (titanium and tantalum) carbide tools has been witnessed. Because of lack of proper toughness, cemented carbides are not suitable for cutting tools such as drills and certain other tools with complex geometry.

Most of the complex cutting tools are made of one or the other grade of high speed steel. High speed steel tools usually fail by progressive wear on the tool. The tool wear can be usually seen in two places; the flank of the tool and the rake (top) face of the tool. The former is called flank wear and the latter crater wear. The different contradicting

mechanisms of wear proposed by many investigators will be discussed in the next chapter. Whatever may be the mechanism of wear, minimization of wear progression rate and thus increasing tool life is a desirable feature for the user of the cutting tools.

The objective of this research was to study the effect of titanium carbide coating, obtained by ion plating and subsequent heat treatment, on the life of high speed steel tools. In the present study, prehardened and ground high speed steel (AISI M-1) tools were ion plated with titanium and heat treated in vacuo to convert titanium to titanium carbide. The titanium carbide thus obtained was identified by X-ray diffraction and the chemical composition of the coating was determined with Electron Probe Micro Analysis. The coating composition variation with coating depth was obtained by analyzing characteristic Auger electrons of the elements after sputtering away layers of atoms at twenty second intervals. Tool life experiments were designed and conducted in order to evaluate the performance of the coating on the life of high speed steel tools.

The experimental details, the results and the conclusions are presented in the following chapters.

CHAPTER II

LITERATURE REVIEW

In Chapter I, a brief introduction to the development of cutting tools and a summary of this research were presented. In this chapter, the related literature will be reviewed. The literature is reviewed under two broad categories; namely metal cutting tools and coating technology. Under metal cutting tools the different forms of tool wear and the wear mechanisms involved are discussed. The different processes for obtaining thin films and the mechanisms involved are discussed under coating technology.

Metal Cutting Tools

"Human progress has gone step by step with the discovery of better materials of which to make cutting tools, and the history of man is therefore broadly divisible into the Stone Age, the Bronze Age, the Iron Age, and the Steel Age."[5] Quite obviously cutting tools have clearly had a very important effect on the progress of mankind. Among metal-cutting tools used are high carbon steel tools, high speed steel tools, cemented carbide tools, ceramic tools, to some extent diamond and cubic boron nitride tools.

In metal cutting the workpiece material ahead of the tool cutting edge is plastically deformed at very high strain

(1 to 2 in/in) and strain rate (>10^4 per second) and much of the energy input is transformed into heat. The heat generated flows into the chip, the tool and the workpiece and the hot chip slides over the tool rake face. After the tool has been in use for some time, a wear land will appear at the flank of the tool below the cutting edge extending parallel to the cutting edge. The wear will also be seen on the tool rake face forming a characteristic cavity known as a "crater" which begins at a distance from the cutting edge as shown in Figure 1. The useful life of a tool is limited by the amount of tool wear which would increase the surface roughness and decrease the cutting efficiency. Hence tool wear is a deciding factor for tool life. Consequently the study of tool wear and methods to improve wear resistance of the tool are essential for improved tool life.

The mechanisms of tool wear can be broadly classified into three categories as follows:

1. Adhesion Wear
2. Diffusion Wear
3. Abrasion Wear

A limited amount of review of these mechanisms is presented in the following sections.

Adhesion Wear

Adhesion wear is based on the concept of the formation of welded junctions and the subsequent destruction of these.

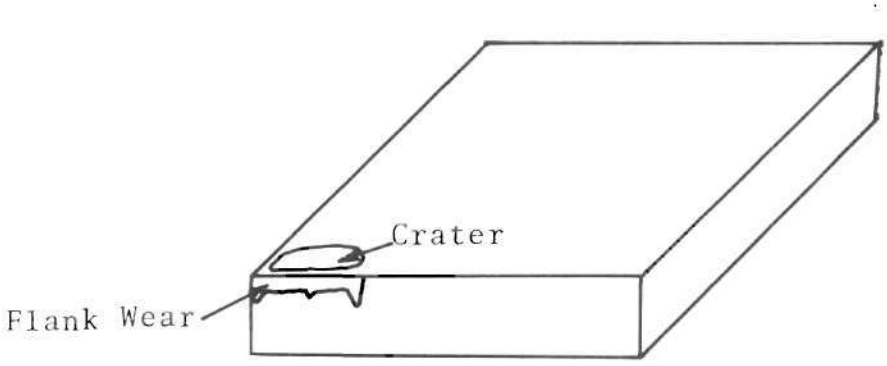

Figure 1. Tool Insert

In metal cutting, junctions formed between the tool and the chip are fractured and small fragments of the tool material can be carried away on the underside of the chip or on the workpiece surface. Merchant, Ernst and Krabacher,[6] in their studies using radioactive tools for rapid tool life testing, concluded that major portions of the wear debris were transferred to the chips. They reported that when AISI 8650 steel was turned with sintered carbide tool, 95.8 percent of the wear products, both top and flank adhered to the chip.

Shaw and Dirke[109] applied adhesion wear theory to wear land formation on a cutting tool and explained the growth of the wear land on the clearance face. They observed that when plotted against time, the wear land grew in three different stages. An initial region of rapid wear, then an approximately constant wear-rate region, and finally a rapid wear region.

Trigger and Chao[7] examined the wear of cemented carbide tool top surfaces and found that wear at the top surface is essentially of the transfer type and the formation of crater wear is strongly temperature dependent. Crater wear for a given tool-work combination, in their opinion, can be correlated with tool-chip interface temperature in a manner predictable from simple laws of adhesion wear in combination with the theory of rate process.

Dawihl[8] reported that mutual diffusion of materials at a particular "adhesion temperature," causing welding of

certain constituents is the main reason for adhesion and transfer type of wear.

Diffusion Wear

Solid state diffusion occurs when atoms in a metallic crystal move from a region of high atomic concentration to one of low concentration. The diffusion process is dependent on the temperature, and the rate of diffusion increases exponentially with temperature increase. In metal cutting high temperatures exist and it is possible for atoms from tool material to diffuse into the work material or the chip. Because of the atomic diffusion from tool to work material or chip, the tool surface is weakened and this effect is known as diffusion wear.

Wear through mutual diffusion at the tool chip interface has been investigated by several research workers. During the machining of mild steel with high speed steel tools a built-up-edge is formed at the tip of the cutting tool. Venkatesh[9] reported the presence of a very thin "white layer" between the tool and the built-up-edge when observing a section of the tool perpendicular to the rake face under a microscope at magnifications greater than 1500 diameters. He analyzed the white layer with an electron microprobe and concluded that the presence of cobalt in HSS tools retards the formation of the white layer. Opitz and Konig[10] also observed a white layer on carbide tools.

Cook[11] observes that in tool wear the individual wear particles are generally very small compared to those from "conventional" wear and often probably of atomic dimension. In the case of crater wear of HSS tools, he concludes that HSS tools decarburize either low or high carbon-steel. Thus he rules out the diffusion of carbon from the tool into the chip. However, the explanation he provides is that the iron atoms in the tool diffuse into the chip material as it moves over the tool face. The chip material is in the process of deformation and will contain a great many potential sites for diffusion of iron atoms, many more than the tool will have for reverse diffusion. Diffusion is a time dependent phenomenon and the time for which the chip is in contact with tool is very short. Therefore it does not appear to be realistic to attribute a great many iron atoms from the tool to diffuse into the chip.

Wright and Trent[12] investigated the wear mechanisms and processes for high speed steel tools in machining steels, cast iron, and a nickel based alloy. They reported that they observed white layer formation in cutting BSS En 8 (AISI 1040) steel at 33 m/min (100 ft/min) and 0.32 mm (0.0125 in) per revolution feed and that carbon and chromium are diffusing in from the tool. This is in contradiction with the observation of Cook.[11]

Systematic static diffusion tests were conducted between carbide tools and various ferrous metals by Narutaki

and Yamane.[13] The results obtained were that Co, C and W diffuse from the tool into work material, while Fe diffuses from the work to the tool. Narutaki and Yamane[14] conclude that Co diffuses from the tool to the work and Fe diffuses from work to the tool in machining ferrous metals with carbide tools.

Zhilin and Tkachev[15] critically examined the role of diffusion in the wear of cutting tools and conclude that even at cutting temperatures of 1000-1120 C the diffusive component of the total wear of the carbide tool is insignificant. They also confirm that the wear products of the carbide tool when machining steels have the form of separate particles. Also they could remove up to 20 percent of the wear products by washing the chips in acetone, which would indicate that the bond between the chip and the wear particles is weak.

Traditionally it has been reported in the machining literature that diffusion is a dominant mechanism of tool wear.[10,11,12] The wear debris are found to be discrete in nature.[6] It is evident from the results of Zhilin and Tkachev[15] that the bonding between the chip and the wear particles is weak. Hence diffusion bonding between the chip and the wear particles appears to be unlikely. Moreover, Ramalingam et al.[112] rightly point out the weaknesses of diffusion as being not able to explain the tool life scatter and the discreteness of wear debris. In the light of

the above, it does not appear that diffusion is a dominant wear mechanism.

Abrasion Wear

Abrasive wear occurs if a hard particle cuts or grooves one of the rubbing surfaces. The first criterion for appreciable abrasive wear is that the particle should be harder than the surface being abraded. In metal cutting situations there are two sources for hard particles. One is fragmentation of the built-up-edge which is strain hardened chip material and the other is hard inclusions in the work material. The main contribution of abrasive wear is due to hard inclusions in work materials. The rate of wear depends upon the size, shape, hardness and the number of inclusions. Hard carbides, oxides and nitrides are present in many steels, in cast iron and in metal-based alloys.

Recognizing the fact that tool life variation is mainly due to variations in the work material, Ramalingam et al.[16] approached the tool wear problem from the work material view point and identify abrasive wear to be the most probable dominant mechanism of tool wear. In view of the fact that diffusion wear is not able to account for tool life scatter, they rule out diffusion as a significant wear generation process. On the basis that adhesive wear is unable to account for poor bonding between the wear debris and the chip (found by Zhilin and Tkachev[15]) they question

the adhesive mechanism of tool wear.

The abrasive wear mechanism as proposed by Ramalingam et al. can be substantiated in the following manner. The experimental evidence demonstrates that tool wear in machining occurs by detachment of discrete wear debris from the tool. The dimensions of those wear particles transferred depend on the cutting conditions and the dimensions of the hard particles in the tool matrix. In this wear mechanism the wear debris production events are the encounters between the hard phase inclusion particles and the tool surface. Inclusion encounter frequency depends both on the volume fraction of the hard phase and on the particle size of the hard phase inclusions.

In support of the proposed abrasive wear mechanism, machining experiments have been performed on known work material containing known hard inclusions under well defined cutting conditions. The experimental results indicate that the increase in volume fraction of silica increased the wear. Also for a fixed volumetric content of hard second phase particles wear increases with decreasing particle size. This is because of the increase in frequency of the encounters of the hard particles with the tool surface. The principles of conceptual design of ferrous alloys for machinability are developed and experimental evidence is presented to support the alloy design principles.

Byrd and Ferguson[17] conducted a feasibility study using a powder metallurgy technique to examine the effect of hard

particles on carbide tool wear in single point turning tests. Two nominal sizes of Al_2O_3 particles (1 μm and 25 μm nominal dimension) each at the 2 volume percent level were examined in 1020 and 4620 powder metallurgy (P/M) slugs which had been hot forged to full density. They conclude that flank wear depends on nominal particle size, with larger particles giving greater wear and crater wear is independent of particle size but depends only on volume fraction. These results clearly support the abrasive wear model.

From the above review it is clear that not only the tool materials but also the work materials need proper attention to improve machinability. In the light of the experimental evidence provided, the abrasive wear mechanism is able to explain the tool life scatter, flank wear and crater wear and seems to be the dominant wear mechanism in cutting tools. Even from an intuitive viewpoint, when two metals have a sliding contact abrasive wear is bound to occur.

In a recent study of new types of cutting tool, Gane[64] compared the performance of four new types of tool with that of tungsten carbide. During an interrupted cutting test at a cutting speed of 183 m/min, he observed a rapid increase in both crater wear and flank wear in the case of tungsten carbide tool with 10 μm thick titanium carbide coating. This rapid increase in wear rate was attributed to the coating breakdown after a limited time (about 10 minutes).

Tool Life

In production machining operations tool life (tool wear) is a factor of major importance in the process economics. Because of inadequate understanding of the physics of the metal cutting process and tool wear mechanism, adequate tool life and tool wear models have thus far not been developed from the process physics. It will be seen from the previous review that a considerable amount of disagreement exists as to which wear mechanism is predominant under different conditions. Therefore extensive experimentation and evaluation of tool life parameters have been developed (as originated by Taylor).[83]

Tool life testing requires a considerable number of tests if a reasonable functional relationship is to be established between the tool life and cutting speed, feed and depth of cut. The single variable at a time approach used in tool life testing is time consuming and ignores the interactive and second order effects of the variables. Hence the experiments must be carefully planned and executed for proper statistical analysis and model building.

In the model building step, the researcher can make use of certain statistical methods termed Response Surface Methodology (RSM) developed by Box and Wilson[84] and later applied to tool life testing by Wu.[85] During the tests conducted by Wu,[85] flank wear was chosen as a tool life criterion. Apart from variation in tool life due to

measurement difficulties alone, the amount of flank wear that is the tool life shows an inherent variation for identical cutting conditions. Some more examples of the statistical techniques used in tool life evaluation are presented in the following paragraphs.

Taraman and Lambert[87] made use of Response Surface Methodology in the selection of machining variables namely cutting speed, feed and depth of cut while turning SAE 1018 cold rolled steel with tungsten carbide inserts. More recently Subbarao and Jacobs[88] applied nonlinear goal programming (NLGP) to arrive at optimum cutting conditions taking into account the existence of multiple objectives namely metal removal rate, tool life, cutting force and surface roughness and assigning priorities to these objectives. Williams and McGilchrist[89] used RSM in an experimental study of drill life.

Devor, Anderson and Zdeblick[96] investigated the inherent variation of tool life over a range of cutting conditions for a finish turning process. It was reported that as the mean tool life increased, the variance also increased and the respective increases were not in direct proportion with each other. Hence tool life distributions with fixed variance do not appear to model the tool life properly.

The problem of wear of grinding wheels is also amenable to statistical models. Recently Deutsch and Wu[110] analyzed the wear caused by grinding wheel-workpiece interaction by

empirical stochastic models. This type of technique may be relevant to tool life modeling because of inherent variation in tool life.

Of course, there are some limitations of the statistical approach to model tool life. Metal cutting process is not suitable for continuous variation of all the cutting variables, namely cutting speed, feed and depth of cut. Also there can be considerable variation in work material and tool material from batch to batch.

Recently Ramalingam et al.[91,92,111,112] addressed the problem of tool life distributions. Tool life models were developed using probability theory.[91,92] Tool life was identified to be stochastic in nature and the tool life models developed portray tool failure as resulting from injuries due to damage producing encounters in machining. For a single injury (tool fracture) model, the tool life was shown to follow a Weibull distribution,[91] where as for a multiple injury failure model, tool life distribution was shown to be log-normal.[92] The single injury failure model presented from a mechanistic viewpoint was later experimentally validated in interrupted cutting test. The stochastic encounters between the refractory nonmetallic inclusions in steel and the carbide particles in the tool were identified to be responsible for the distributed tool life.[112] It was shown that the mean tool life can be increased by decreasing the encounter frequency but this will lead to an increase in tool life

scatter. They conclude that distributed tool life is inherent to the machining process.

The above tool life models presented on a physical basis are able to explain the tool life scatter. However, along with a better understanding of the mechanics of machining, a more exact tool life model is awaited.

Coating Technology

The wear resistance of cutting tools may be improved either by working with the bulk of the tool or by increasing the wear resistance of the surface of the tool. The wear resistance of the surface can be enhanced by surface heat treatment and/or by depositing a wear resistant layer on the surface of the tool. In industrial practice it has long been reported that the titanium carbide (TiC) coated tools perform better than the solid TiC tools. The TiC coating on cemented carbides is usually obtained by Chemical Vapor Deposition (CVD).[42] Recently an excellent review of chemical vapor deposition and its application to protective coatings on metals has been done by Yee.[67]

Complex tools like drills, end mills, gear shaping cutters and gear hobs are largely manufactured of high speed steel. Thus the tool wear improvement in case of high speed steel is important and this may be achieved by having a wear resistant thin film on tough high speed steel substrate.

In any thin film deposition process, it is desirable

for the deposition to be performed in a vacuum so that the contamination of the film is kept to a minimum. It has been a common practice for some time to obtain vacuum deposited coatings. In this, the material to be deposited is vaporized in a vacuum and condensed so that the condensed solid film sits on the substrate (the material to be coated). The energy imparted to the evaporated atoms is not enough for any embedding or implantation of atoms to take place. A better way would be to give more energy to the atoms of the target material. This is essentially the idea behind sputtering involving glow discharges. These sputtering type processes may be classified into three broad categories.

1. Sputtering
2. Ion Plating
3. Ion Implantation

1. Sputtering

Sputtering is again divided into DC (Direct Current) sputtering or RF (Radio Frequency) sputtering depending upon the power supply, used for sputtering purposes.

DC Sputtering. The schematic diagram of the discharge tube is shown in Figure 2. When the voltage across the electrodes in a discharge tube at low pressure is increased, the electrons emitted from the cathode collide with the atoms or molecules of the low pressure gas, thus transferring the energy to the atoms and hence ionizing the atoms or molecules. When the ionization level is high enough, there will be a

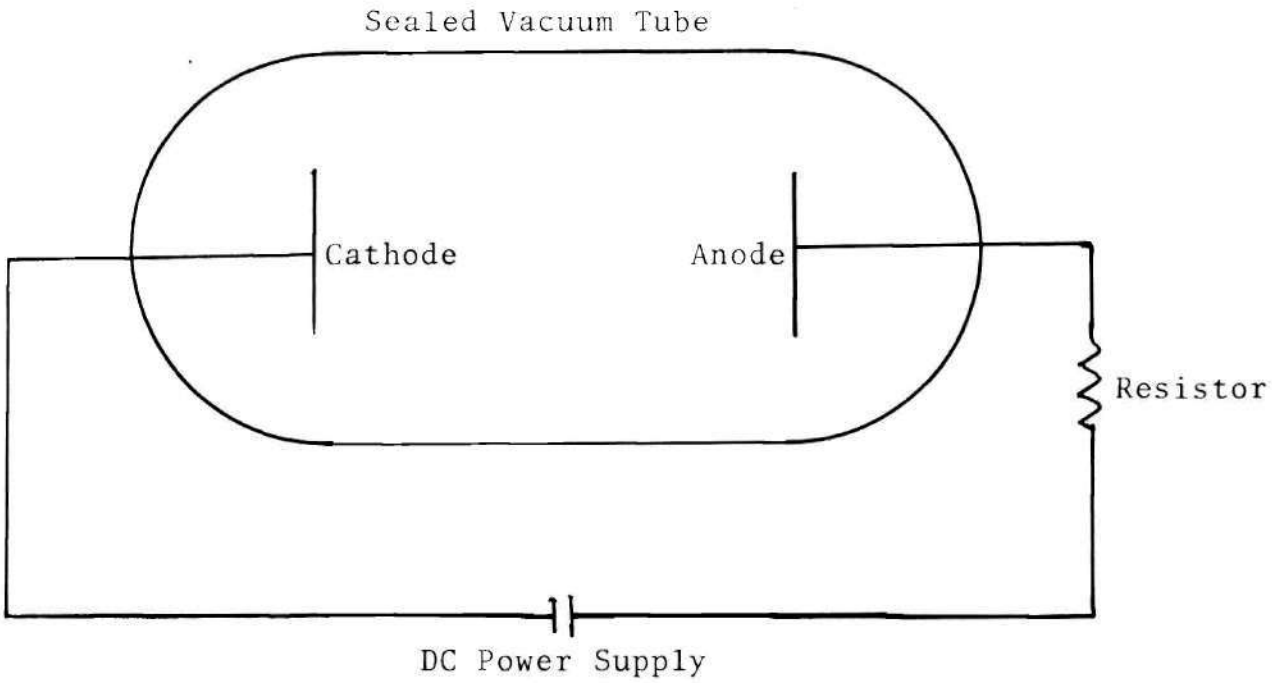

Figure 2. Discharge Tube

glow discharge and the tube conducts. The gas, if it is in a highly ionized state containing electrons, ions and neutral atoms and molecules, is called a plasma. Once the ionization starts, the potential required for maintaining the ionization is relatively small.

The ions are attracted by the cathode because of the potential across the electrodes: the energetic ions thus are slightly accelerated and impact the cathode and knock the atoms off by transferring the momentum. These atoms travel with that momentum and eventually reach the anode and get deposited. In the travel it is likely that some of these target (cathode) atoms may be ionized.

RF Sputtering. In this method a radio frequency (RF) power supply is utilized to create the same type of plasma as in DC sputtering but due to the improved frequency by a matching network in the field, non-conducting substrates can be coated.

Reactive Sputtering. Reactive sputtering can be defined as sputtering in the presence of a reactive gas so that the deposited film has a different chemical composition than the target material. To form carbides and nitrides, the reactant source is either a carbon containing gas (e.g. C_2H_2) or nitrogen (N_2). It is also possible to vary the non-metal to metal ratio by varying the partial pressure of the reactive gas (argon + nitrogen or argon + methane).

Hrbek measured,[18] in situ, the sputtering yields of Ti,

Ta, Mo and W bombarded by Ar ions (by a weight loss measurement) as a function of the partial pressure of reactive gas (O_2 or N_2) and he is of the opinion that the sputtering yield in the presence of a reactive gas is lower because the reactive sputtering mechanism is controlled by the adsorption-sputtering mechanism of the reactive gas adsorbed, by changes in the surface binding energy due to adsorption and finally by collision mechanics. Shinoki and Itoh[80] investigated the mechanism of RF reactive sputtering by mass spectrometry and conclude that the reaction process can be strongly influenced by the gettering action of the sputtered atom deposits.

Greene and Pestes[19] used DC biased RF sputtering to deposit adhesive TiC and TiVC films on AISI T-15 high speed steel substrates. The film thickness ranged from 1500 Å to 1.4 μm. The target materials were TiC and TiVC pressed discs of 4 inches diameter and 1/4 inch thick. They report that the most adhesive film was deposited under conditions of the highest substrate temperature and bias used in these experiments, 300°C and -500V DC, respectively.

Su and Cook[20] employed RF reactive sputtering for the coating of AISI T-1 and AISI T-15 high speed steel tools with 4 to 5 μm thick titanium nitride layer. Most of the sputtering was done with the substrate at the ground potential, 4-10 micron argon pressure, and at 750 RF watts with corresponding target potential of 3150 volts. The usual deposition time they report as 5 hours for a layer

thickness of 4-5 μm. The tool life has been reported to have improved 2 to 4 times. The only disadvantage is that it is a very slow process (the deposition rate is about 1 μm per hour).

Sollenberger[59] reported the production of titanium nitride coating on a carbide (94WC-6Co) substrate by reactive sputtering. Results indicate excellent adhesion of the coating to the substrate and no crater wear on the coated tool when the tool was used for four minutes and thirteen seconds in turning AISI 1045 at a surface speed of 106.7 meters per minute. Uncoated carbide tool under the same conditions showed a crater depth of 57.4 μm. The coating deposition rates reported are 30 to 60 μm per hour which appear to be very good.

2. Ion Plating

Ion plating was originally developed by Mattox[21] and has been used by many in different variations for different purposes. Ion plating is an improvement over sputtering in the sense that a separate source for evaporation of target material is provided. These target atoms have a finite probability that they will be ionized. The magnitude of this probability is a function of the ionization potential and the temperature of the atoms. If the vaporized (metal) atoms are ionized in the space between the source and the substrate, they have an excellent chance of reaching the substrate as ions. If the substrate is electrically

(negatively) biased, therefore these ionized atoms are accelerated to the substrate and get deposited.

Teer[61,62] discussed the reasons for good adhesion of ion plated films and related the energies of particles in a glow discharge to the ion plating process. Teer reports that he was unable to cause an adhesive failure of ion plated films. Reasons for the high adhesion reported by Teer[61,62] are as follows.

1. In ion plating the substrate is cleaned prior to plating and is maintained clean during plating by the ion bombardment.
2. The deposition takes place in the discharge.

It is believed that the vapor atoms are ionized and arrive at the substrate with high energies thus penetrating the lattice of the substrate. Even if the ions arrived at the substrate with a maximum possible energy, i.e. 5 keV in a 5 kV discharge, the maximum depth of penetration would be very small, about 50Å. However, in ion plating, the initial cleaning by ion bombardment which removes adsorbed gases and contaminants that could act as barriers to diffusion and the formation of high density of defects in the surface layers, are responsible for promoting diffusion.[66]

Aisenberg and Chabot[22] discussed some of the physical mechanisms involved in ion plating. The important processes associated with ion plating suggested by them are as follows:

1. evaporation of the deposition material into moderate vacuum (in the micron range)

2. gas collisions of the deposition material to give diffusion, scattering, and covering of hidden surfaces
3. agglomeration of some of the deposition material into small clumps
4. negative charging of these small clumps as a result of the plasma present in the deposition chamber
5. repulsion of these negatively charged clumps from the negative deposition substrate (this removes the tendency to form granular deposits)
6. positive ion bombardment of the substrate to increase the average energy of surface atoms to make them mobile enough to move into better crystallographic sites and to give non-porous film and better adhesion
7. positive ion bombardment of the substrate to remove gas atoms and give better film adhesion.

Bunshah et al.[23,24,65] developed a process called Activated Reactive Evaporation (ARE) which is essentially ion plating with electron beam evaporation instead of thermal evaporation. Electron beam evaporation, as the name indicates, makes use of an electron beam for evaporation. The electron beam is a stream of energetic negatively charged particles. In electron beam evaporation the beam is directed on the top surface of the target material in a vacuum environment. When an electron beam is used as the source of

heating, deviations from the equilibrium population of ions can be achieved. As the primary electron beam passes through the vapor cloud directly above the source, ion-pairs (electron, positive ion) are created by the collision of vapor atoms with the high energy electrons. When they are accelerated to the substrate their energy impact contributes substantially to deposit adhesion.

Reactive ion plating, where ion plating is done in a reactive atmosphere, enables one to deposit compounds such as carbides and nitrides. Zega et al. have obtained gold colored hard coatings of TiN on carbon steel, stainless steel and Stellite[25] substrates by ion plating titanium in an atmosphere of nitrogen. The titanium evaporation source was heated by a 90° deflected electron beam obtained from a cold-cathode discharge gun. Deposition rates up to 500 $\mathring{A}\ min^{-1}$ have been obtained. They report that abrasion tests performed on coated pieces showed excellent resistance to abrasion.

Bunshah and Shabaik[23] utilized the ARE process to coat TiC on high speed steel (M-43) at a substrate temperature of 500 C. They report that tool life improvement by a factor of 3 and a reduction in tool force and tool tip temperature by a factor of 2 in machining AISI 4340 steel.

Kodama, Shabaik and Bunshah[54] studied the cutting performance of cemented carbide tools coated with hafnium nitride (HfN) and titanium carbide (TiC) by the ARE process and reported that the flank wear rate of the TiC-coated tools

was less than that of the HfN-coated tools. It is concluded by the authors that carbides could be more useful compounds than nitrides in terms of flank wear.

Hill et al.[26] investigated the use of electron beam evaporation of a metal in a reactive atmosphere to produce refractory compounds like TiN, TiC and ZrN. They conclude that there may be a rate of evaporation (and deposition) above which the ARE process is inoperative.

Stowell[27] made TiC coatings on steel and Ti substrates by reactive ion plating using an electron beam evaporant source in an ethylene plus argon gas mixture. All the coatings required a post heat treatment to convert titanium and carbon to titanium carbide.

Nakamura et al.[28] report that there are several physical vapor deposition processes being developed in Japan to obtain hard refractory carbide and nitride thick films. They have obtained TiC coating on cemented carbide tips using a low pressure plasma deposition (LPPD) process which is a variation of the ARE process. The deposition rate of titanium carbide was 1 to 2 μm min^{-1} and the electron beam power was 10 kV X 200 mA. The optimum film thickness for flank wear resistance and for crater wear resistance are reported by this group to be 2 to 4 μm and 3 to 10 μm respectively. They have also reported coating of TiN and the use of hollow cathode discharge (HCD) process for hard chromium platings.

3. Ion Implantation

Ion implantation is the process of modifying the properties of a solid by embedding into it appropriate atoms in the form of a beam of ionized particles. In ion implantation, the ionized particles are first separated from the impurities and then accelerated to hit the substrate and penetrate into the substrate. Ion energies involved vary between 20 keV and 5000 keV and the typical beam currents generated are in the range of a few micro amperes to several hundred amperes depending on the mass of the ion. The depth of implantation depends on the mass and energy of the implant species and the nature of the substrate.

Ion implantation was originally used for semiconductors but recently it is finding place in anti-wear and anti-corrosion applications.[53] Hartley[29] observed large changes in friction coefficient (up to 60%) on steel surfaces implanted with such ions as Pb^+ and Sn^+. He also reports that implantation of boron, nitrogen and molybdenum reduces wear by more than a factor of 10 from measurements with a pin and disc machine.

It is possible to obtain a wear resistant layer by implanting Ti^+ and C^+ but the depth of penetration as well as the coating produced is only a few hundred angstrom units which is a thin layer for enhancing the wear resistant cutting tools. It is also expensive and may be inadequate for tool wear applications. The role of ion implantation as

an intermediate or preparatory technique to produce an interfacial layer may be important.[30]

CHAPTER III

EXPERIMENTAL PROGRAM, TECHNIQUES AND PROCEDURES

From the literature reviewed, it appears that ion plating and sputtering are likely candidates for use in the case of high speed steel tools to obtain wear resistant thin films. But sputtering is a very slow process as is evident from the results of Su and Cook.[20] Thermal energies of vaporized particles are on the order of 0.1 eV. In sputtering, particle energies are far greater than thermal energies and can be as high as 100 eV. In ion plating since a separate source is used for evaporation in a glow discharge the depositing metal ions may have higher energies. Ion plating thus is believed to produce a composition gradient at the interface because of sputter cleaning prior to and during deposition and defect creation in the surface layers to enhance diffusion. In the present study, ion plating along with subsequent heat treatment was used to obtain wear resistant coating of titanium carbide on high speed steel (AISI M-1) tool substrate.

Titanium carbide when coated on cemented carbide tools improved the wear resistance of the tools because it creates less friction between the tool rake face and the chip. At the same time TiC costs 100 times less than cubic

boron nitride (Borazon, trade name of General Electric) or diamond, which is a considerable economic incentive. TiC is believed to cause the formation of a titanium oxide surface layer that effectively isolates the tool from the part to be cut and in a sense, protects the tool from rapid wear. The refractory carbides and nitrides are not primarily stoichiometric phases.[33] Different processing techniques tend to produce different defect structures and hence different properties. Recently Ramalingam[31] examined the dependence of mechanical properties of titanium carbide on stoichiometry and showed that the superiority of the coated carbide tools is probably due to near perfect stoichiometry obtained by chemical vapor deposition process.

Titanium[32] (atomic number 22) is a silver-grey metal with a density of 4.5 gms/cm^3 and a melting point around 1670 C. It is about as strong as steel yet only half as dense; however, its strength and resistance to corrosion drop rapidly above 800 C; at higher temperatures the massive metal reacts with oxygen, nitrogen, carbon, and boron to give TiO_2, TiN, TiC and TiB_2. The ground state outer electronic configuration of titanium is $3d^2 4s^2$ and the ionization energies are 656 (1st), 1309 (2nd), 2650 (3rd), and 4173 (4th) kJ mol^{-1}. The atomic radius of titanium is 0.132 nm. With light nonmetallic elements B, C, N, and O, interstitial solid solutions are formed. In these solid solutions the light atoms occupy positions in the interstices of the metal lattice. The ratio

of the atomic radii of the nonmetal to the metal needs to be less than 0.59 for interstitial compound formation to occur. Stoichiometric compounds do arise when the available interstitial holes are filled by the light element. Thus, if all the octahedral holes in a face-centered cubic close packed structure are filled, a 1:1 stoichiometry results as in TiB, TiC, TiN, and TiO. Such solid solutions have the rock salt structure. These interstitial compounds are usually hard, of high melting point, and chemically inert.

The structure of TiC is the B1 or rocksalt (FCC) structure and its primary glide system is (111) [110]. The lattice parameter of TiC is 4.3280 and its room temperature hardness observed by Kornilov is 3000 kg/mm^2. The heat of formation of TiC is 43.9 kCal/mol. Its density is 4.938 g/cm^3. The melting point of the carbide is reported to be 3250 C. TiC is reported to exist with the same lattice over a range of chemistries from $TiC_{0.6}$ to $TiC_{1.0}$ indicating a capacity to form stable defect lattices.

Titanium carbide plastically deforms above 800 C on the (111) planes in the [110] direction.[33] Below about 800 C it fails in a brittle fashion. Figure 3 shows ductile-brittle transition in carbides where σ_f is the fracture strength or cleavage strength, σ_y is the yield strength, and T_{DB} is the ductile-to-brittle transition temperature. Below T_{DB} the carbide fractures or cleaves because the stress necessary to produce fracture (σ_f) is lower than the stress needed to move

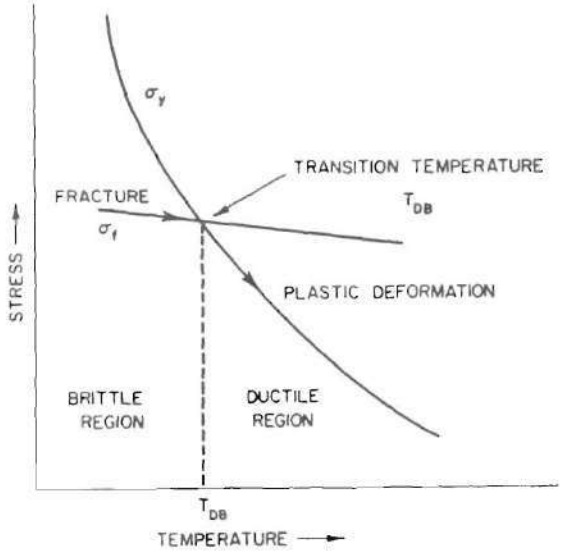

Figure 3. Ductile-Brittle Transition in Carbides[33]

dislocations (σ_y); above T_{DB} the opposite is true and the carbide is ductile.

The fracture strength to some extent depends on the nonmetal to metal ratio.[33] Deviations from stoichiometry will decrease the number of nonmetal-to-metal bonds that must be broken during fracture or cleavage. So it is logical to expect that σ_f increases as stoichiometry increases and as the vacancy concentration decreases. This might eventually alter (decrease) the ductile-to-brittle transition temperature.

Titanium carbide coatings have been shown to improve the life of carbide tools.[42] It appears that titanium carbide coating, on high speed steel might improve the tool life. Ion plating of titanium and post heat treatment might thus be a logical process to obtain wear resistant titanium carbide coating on high speed steel tools. Therefore in the present study a titanium carbide coating was obtained on AISI M-1 high speed steel tools using ion plating and post heat treatment. The experimental details can be divided into the following.

- Ion Plating System
- Preparation of the Tools
- Characterization of the Coated Tools
- Tool Life Testing of the Coated Tools

Ion Plating System

The ion plating system used in the present study is

schematically shown in Figure 4. This system consists of the following items.

1. Vacuum System
2. Power Supplies
3. Coating Chamber
4. Gas Medium

1. Vacuum System: The vacuum system consists of a mechanical pump, a diffusion pump, necessary gages for pressure (vacuum) measurement and a vacuum chamber. The vacuum system must be able to deliver pressures below 10^{-5} torr.

2. Power Supplies: Two types of power supplies are needed for ion plating. One is a variable AC high current-low voltage for resistance heating of the titanium source filament. The second power supply is for the creation and maintenance of the plasma and hence it should be a direct current high voltage-low current type.

3. Coating Chamber: In most cases the vacuum chamber was used as the coating chamber.

4. Gas Medium: A noble gas like argon (A) was used for creation of the plasma and for sputter cleaning the tools before they were ion plated with titanium. For reactive ion plating, a reactive gas, methane (CH_4) is needed so that a mixture of argon and methane can be leaked into the chamber during ion plating. The partial pressures of the two gases have to be properly selected to obtain the desired

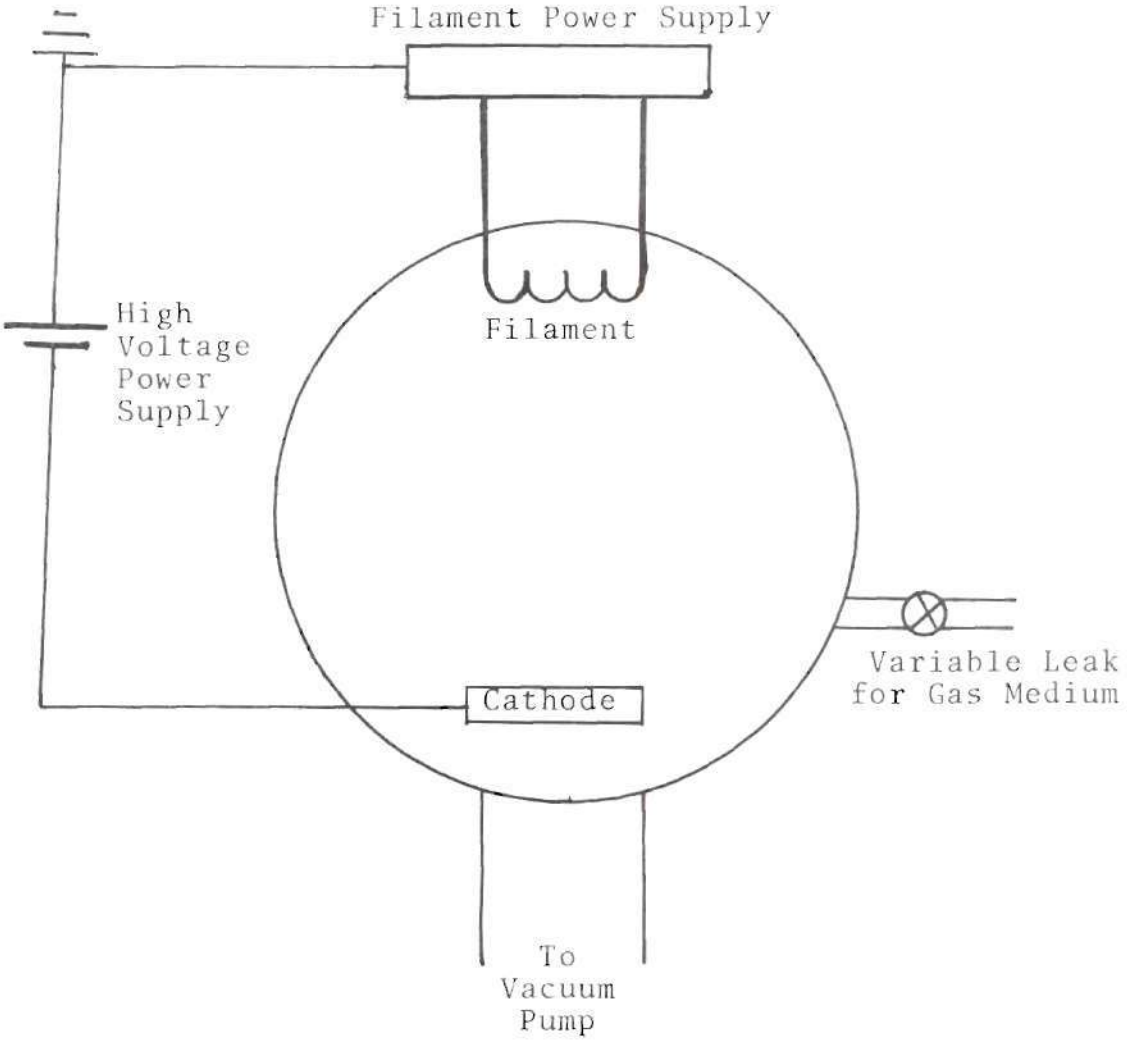

Figure 4. Schematic Diagram of Ion Plating System

compound of titanium carbide.

Preparation of the Tools

Initially rough high speed steel inserts of AISI M-1 type (0.125 + 0.050 in) were sliced from comercially available prehardened and ground 0.500 in x 0.500 in x 4.000 in tool bits using a cut off wheel with slow feed to make sure that the inserts were not burned. The rough inserts were then carefully ground to 0.125 in x 0.125 in x 0.500 in using a surface grinder. A 11° clearance angle was ground on four sides of each insert making use of the grinding fixture fabricated for this purpose. Each insert thus gives four cutting edges at four corners. The nose radius was ground by hand on four corners of each insert with a honing stone. The high speed steel tool inserts were ultrasonically cleaned in acetone and were ion plated by the following procedure.[36]

1. The filament was mounted and the samples placed on the cathode.
2. The vacuum chamber was pumped down to a pressure of about 10^{-5} torr.
3. A small amount of argon was leaked and the chamber was evacuated and this process was continued until the chamber contained only argon.
4. The pressure inside the chamber was maintained at about 16 microns by judicious choice of the argon flow rate and the pumping rate.

5. The high voltage was slowly applied until a pink argon plasma was observed. The specimens were sputter cleaned for about 15 minutes at 2.9 kV and 100 mA.
6. The system was changed to an ion plating mode and the filament was turned on.
7. The plating was carried out in an argon medium for about 3 minutes at 1.4 kV and 150 mA.
8. The high voltage was first turned off, quenching the plasma.
9. Filament current was then turned off.
10. The chamber was allowed to cool for a few minutes.
11. The coating chamber was closed for the vacuum pump.
12. The chamber was opened and the samples were taken out.

Post Heat Treatment of the Tools

The AISI M-1 high speed steel tool inserts coated with titanium in argon atmosphere were hardened in vacuum at about 1200 C for five minutes and then quenched in argon. Two tempers as recommended by the tool steel manufacturer (Latrobe Steel Company), were given to the coated bits following hardening. The first one was for 2 hours at 566 C and then cooled to room temperature. The second temper was for 1.5 hours at 545 C and then cooled to room temperature. Also the uncoated AISI M-1 tools were heat treated in the

same manner and in the same batch to suppress the heat treatment variable in the comparison of tool life.

Characterization of the Coated Tools

The coating obtained on high speed steel inserts was characterized by X-ray diffraction using a Norelco X-ray Diffractometer at 49 kV and 23 mA with Cu Kα radiation. The coating was identified to be titanium carbide by comparing the powder diffraction pattern with that of the standard powder diffraction file. The stoichiometry of the titanium carbide coating on the inserts was determined using an Electron Probe Micro Analyzer (EPMA) (Action Laboratories Inc., Model MS-64). The beam voltage, sample current and spot diameter used were 14 kV, 80 nanoamperes and 30 μm respectively. The Kα, standards used were quartz 1011 crystal for titanium and lead stearate octodecanate crystal for carbon.

The polycrystalline texture within the thin film was analyzed by obtaining (111) and (200) pole figures on a Siemens texture goniometer. General topography of the surface of the coating was observed in a Kwik Scan Scanning Electron Microscope (SEM). The adhesion of the coating was checked by peel test and ultrasonic agitation.

The chemistry of the surface of the coating as well as the cross section of the coating perpendicular to the tool surface was determined by Auger Electron Spectroscope (made by Physical Electronics, Inc., Model 11). This spectroscope is provided with a sputter gun so that layers of atoms could

be sputter removed and then the chemistry of the layers below the surface can be determined. In this manner if the coating is sputter cleaned for 20 seconds certain amount of the thickness of the coating is removed so as to facilitate the chemical analysis of the coating with coating depth from the surface. The sputter removing layers of the coating and then collecting auger electrons each time lends itself to computer control of the cycle. In fact in the present case the computer control available was utilized to monitor the cycle.

The sputtering process may not remove the layers very uniformly and hence the calibration of coating depth is only relative. However, it provides a way of estimating the interface thickness, if any exists.

After an initial scan, the elements, looked for in the coating, were carbon, oxygen, titanium and iron. The primary beam energy was 3 keV at a pressure of 5×10^{-5} torr. The relative amounts of different elements present with sputtering time are presented in Table 2 and the data is plotted in Figure 13.

Tool Life Testing of the Coated Tools

Tool life tests were conducted on an AISI 1045 work-piece of about 4.5 inches in diameter and 30 inches long using AISI M-1 square inserts coated with 0 μm, 2 μm, 4 μm, and 7 μm thicknesses. Machining was done on a Cincinnati 15 inch, 5 hp lathe with Cimcool coolant. The tool holder type

used was the Carboloy (trade name of General Electric Corporation) positive rake and 15° approach angle. Cutting conditions were 175 ft/min or 125 ft/min and feed rates of 0.0025 in/rev, or 0.0075 in/rev with the depth of cut held at 0.060 inches.

For proper analysis and to draw meaningful conclusions, the tool life experiment was designed prior to performing the experiment. There are three variables to be taken into account; cutting speed, feed and coating thickness, and the depth of cut being held constant. A two level, three factor experiment with a center point was found to be adequate within the constraints of the experiment. Because of experimental observation of no difference in performance between 7 μm and 4 μm thick coated tool, the 7 μm thick coated tool was deleted from the experiment. The 2^3 design with center point is shown in Figure 5 pictorially and the details of the experimental points are illustrated in Table 1.

Wear land measurements were taken at 1, 2, 3, 5, 7.5, 10, 12.5, 15 minutes of elapsed cutting time using a microscope at a magnification of about 40X. The average as well as maximum wear land width were measured. The test was interrupted at the above intervals to plot the progression of wear land width with time. Crater depth was measured at the end of 15 minutes of cutting on both coated and uncoated tools using a Bendix profilometer. The results, obtained, are presented in the next chapter.

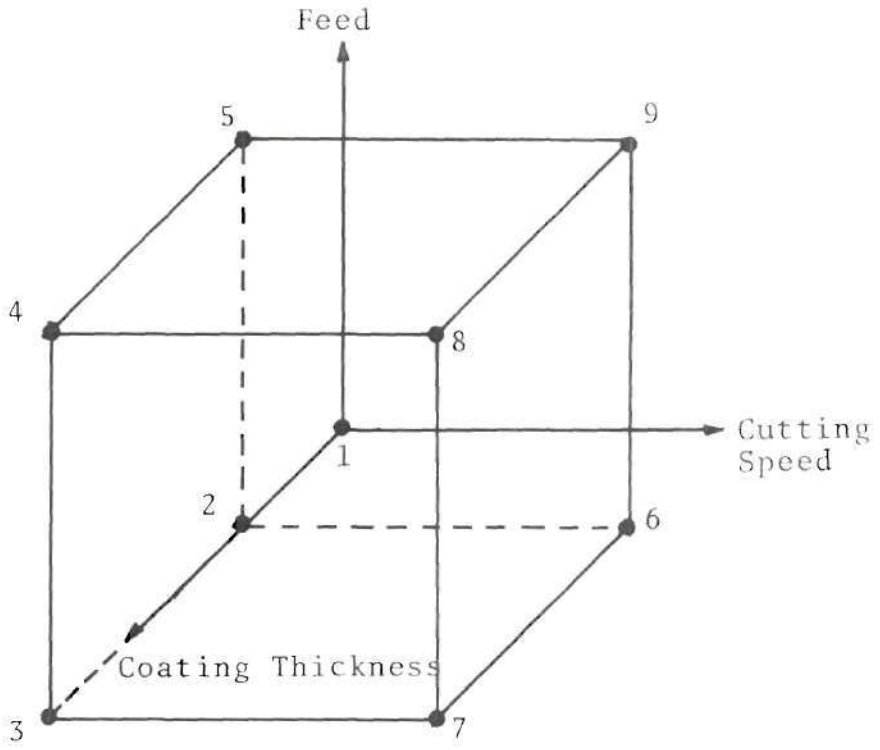

Figure 5. 2^3+ Center Point Design Used for Tool Life Experiment

Table 1. Cutting Conditions for Tool Life Experiments

Test No.	Cutting Speed fpm	Feed in/rev	Coating Thickness µm	Cutting Speed (Coded)	Feed (Coded)	Coating Thickness (Coded)
1	150	.0050	2	0	0	0
2	125	.0025	0	-1	-1	-1
3	125	.0025	4	-1	-1	+1
4	125	.0075	4	-1	+1	+1
5	125	.0075	0	-1	+1	-1
6	175	.0025	0	+1	-1	-1
7	175	.0025	4	+1	-1	+1
8	175	.0075	4	+1	+1	+1
9	175	.0075	0	+1	+1	-1

Depth of cut was 0.060 inch constant for all cutting conditions.

CHAPTER IV

RESULTS

In the present study prehardened and ground AISI M-1 high speed steel inserts were ion plated with titanium and then heat treated to obtain TiC coating. The coating was characterized as to the composition and stoichiometry and then tool life tests were conducted to evaluate the performance of the coated and uncoated tools. The results obtained are presented in this chapter under the following categories:

- Surface Observation of the Tools
- Characterization of the Coating
- Stoichiometry of the Coating
- Texture of the Coating
- Characteristics of the Coating Cross Section
- Work Material Characterization
- Evaluation of the Tool Wear

Surface Observation of the Tools

Scanning Electron Micrograph of surface topography of prehardened and ground AISI M-1 tool insert is shown in Figure 6. The inserts were not polished before coating but they were ultrasonically cleaned in acetone prior to coating. A micrograph of an electropolished and etched AISI M-1 HSS insert is shown in Figure 7. Isometric view of the ion

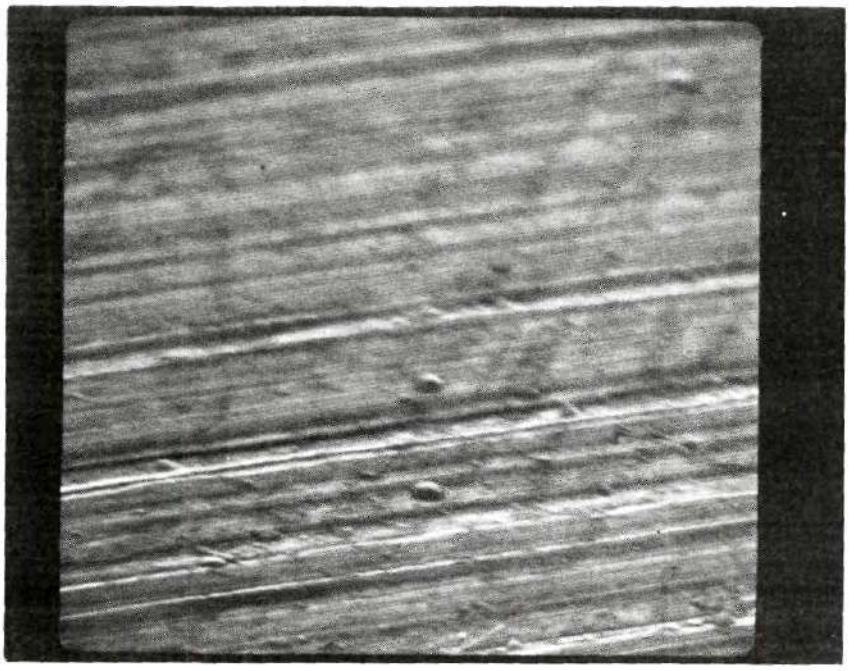

3000X

Figure 6. Scanning Electron Micrograph of Surface Topography of AISI M-1 Tool

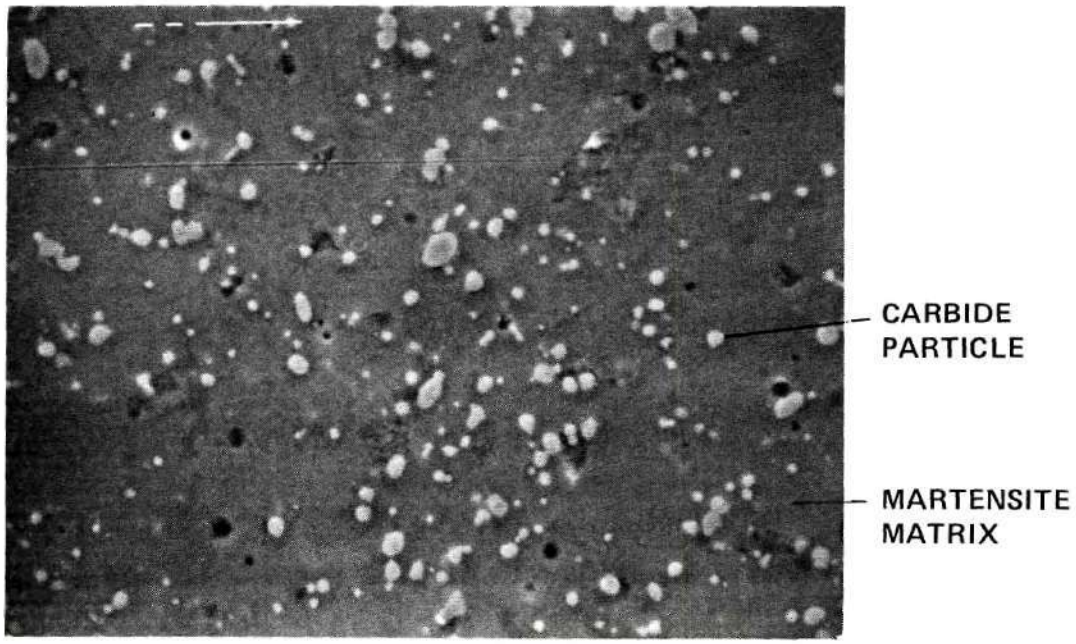

Figure 7. Scanning Electron Micrograph of AISI M-1 Tool Electropolished and Etched

plated and heat treated HSS insert is shown in Photomicrograph 8 at a lower magnification. Figure 9 illustrates the surface of the coated tool at a magnification of 850X. The streaks observed were due to grinding of the specimen prior to coating. The coating appears to be uniform and the dark gray color resembles titanium carbide.

Characterization of the Coating

The powder diffraction pattern for the surface of ion plated and heat treated AISI M-1 tool inserts is shown in Figure 10. The film thickness of the coating on these tools was about 2 μm. The (111) and (200) peaks of titanium carbide are indicated in the figure. As is evident from the figure the peak for titanium oxide is also seen in the diffraction pattern. The diffraction pattern was obtained on a Norelco Diffractometer at 49 kV and 23 mA. The lattice parameter calculated (in Appendix C) is 4.38.

Stoichiometry of the Coating

The chemical analysis of the elements in the coating is given below. The stoichiometry of the titanium carbide in the coating was obtained by using Electron Probe Micro Analyzer (EPMA). It varies from $TiC_{0.88}$ near the corner of the insert to $TiC_{0.93}$ in the center. The calculation of the stoichiometry of TiC from the weight fraction is presented in Appendix A.

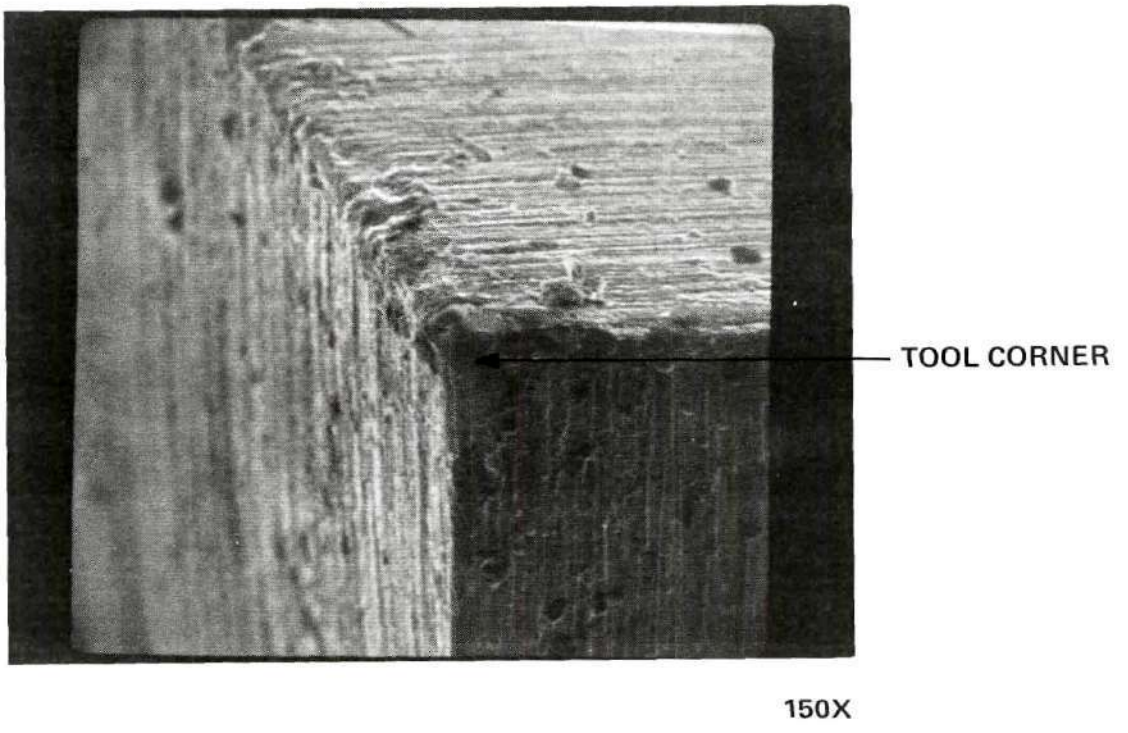

Figure 8. Scanning Electron Micrograph of Isometric View of Ion Plated and Heat Treated AISI M-1 Tool

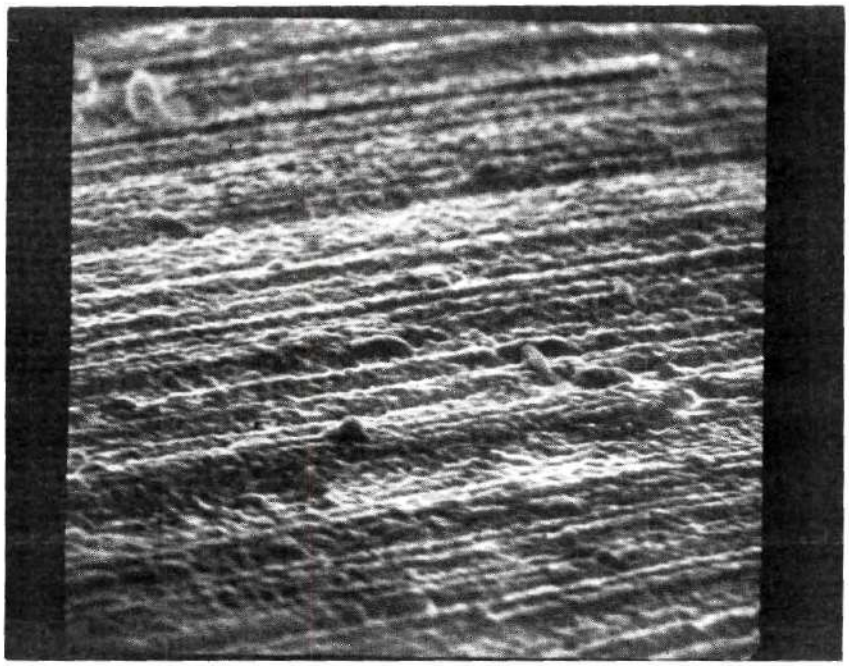

850X

Figure 9. Scanning Electron Micrograph of Surface Topography of Ion Plated and Heat Treated AISI M-1 Tool

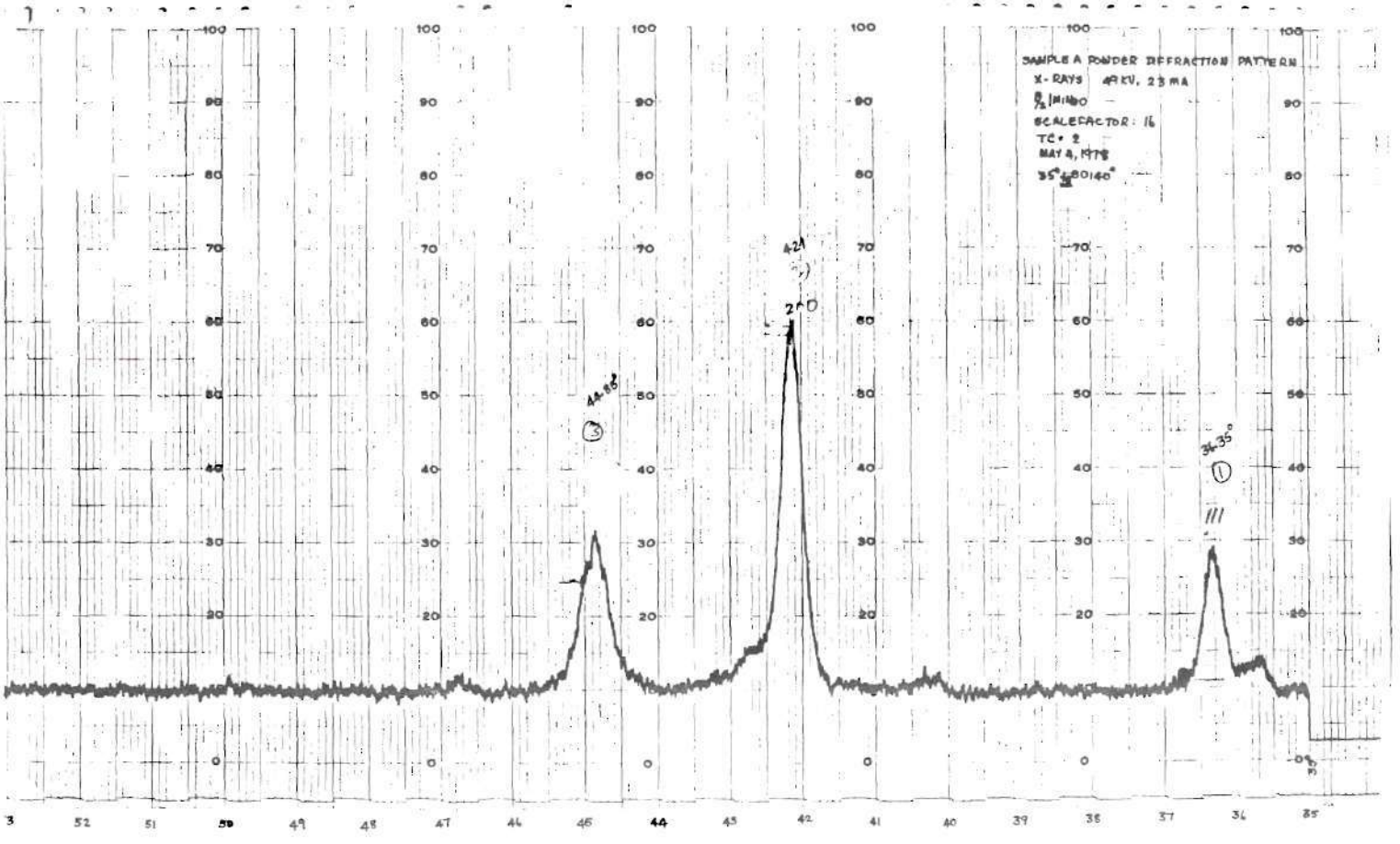

Figure 10. Powder Diffraction (X-ray) Pattern of Coated and Heat Treated AISI M-1 Tool

Texture of the Coating

The pole figures of the titanium carbide coating obtained on the AISI M-1 tool inserts are shown in Figures 11 and 12 of (111) and (200) and were obtained by processing of X-ray intensities measured with the Siemens texture goniometer. A fiber texture with the (100) plane parallel to the substrate was observed.

Characteristics of the Coating Cross Section

The cross section of the coating was analyzed by Auger Electron Spectroscope and the different elements present in the coating are plotted with sputtering time in Figure 13 whereas the data for the figure is shown in Table 2. The stoichiometry of the coating as calculated from the Auger Electron Spectroscope data is (presented in Appendix E) $TiC_{0.88}$ which is slightly less than the value $TiC_{0.93}$ obtained by EPMA.

A fractured cross section of the coated and heat treated AISI M-1 tool insert is shown in Figures 14(a) and 14(b). The coating appears to have a good adhesion to the substrate as is evident from feature (A) in Figure 14.

Work Material Characterization

The work material was a US Steel hot rolled silicon killed fine grain special quality AISI 1045 steel. The chemical analysis of the above work material is given in Table 3. The work material used was a bar of 30 inches in length and 4.5 inches in diameter. A representative sample

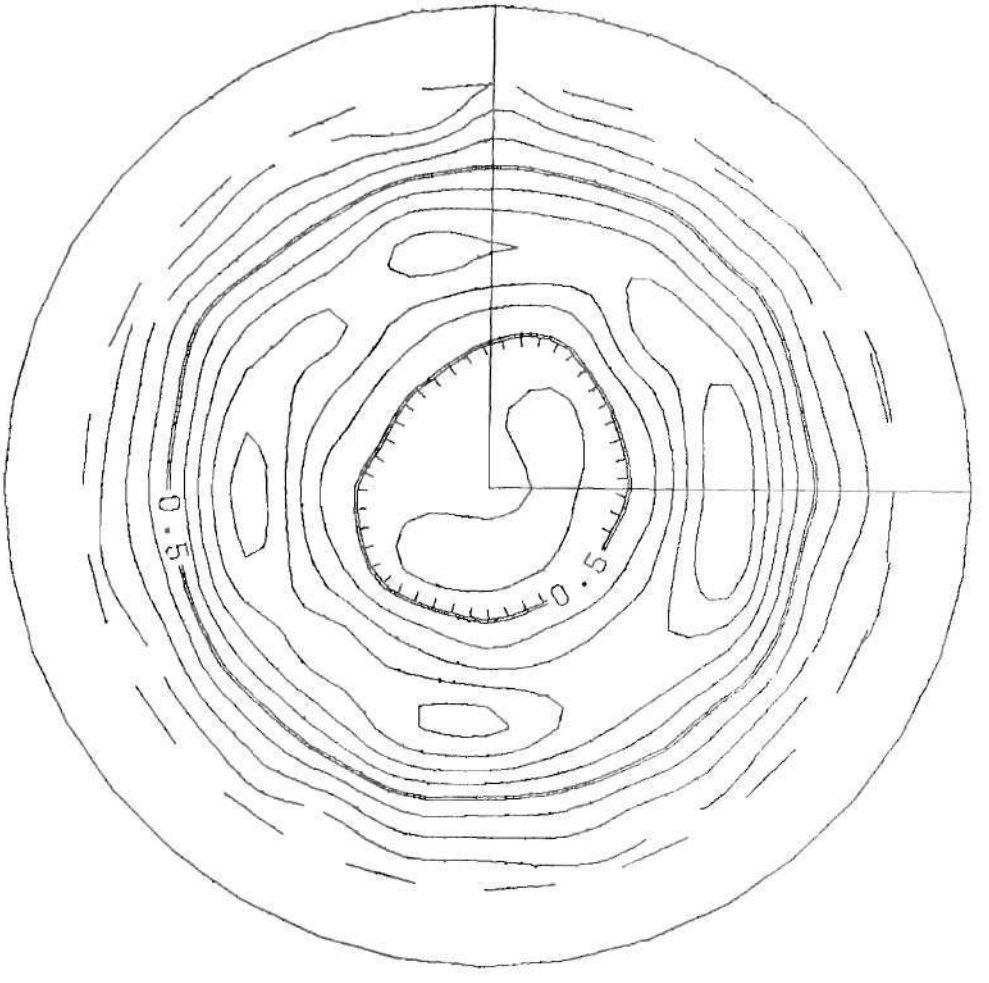

Figure 11. TiC Coating Texture Pole (111)

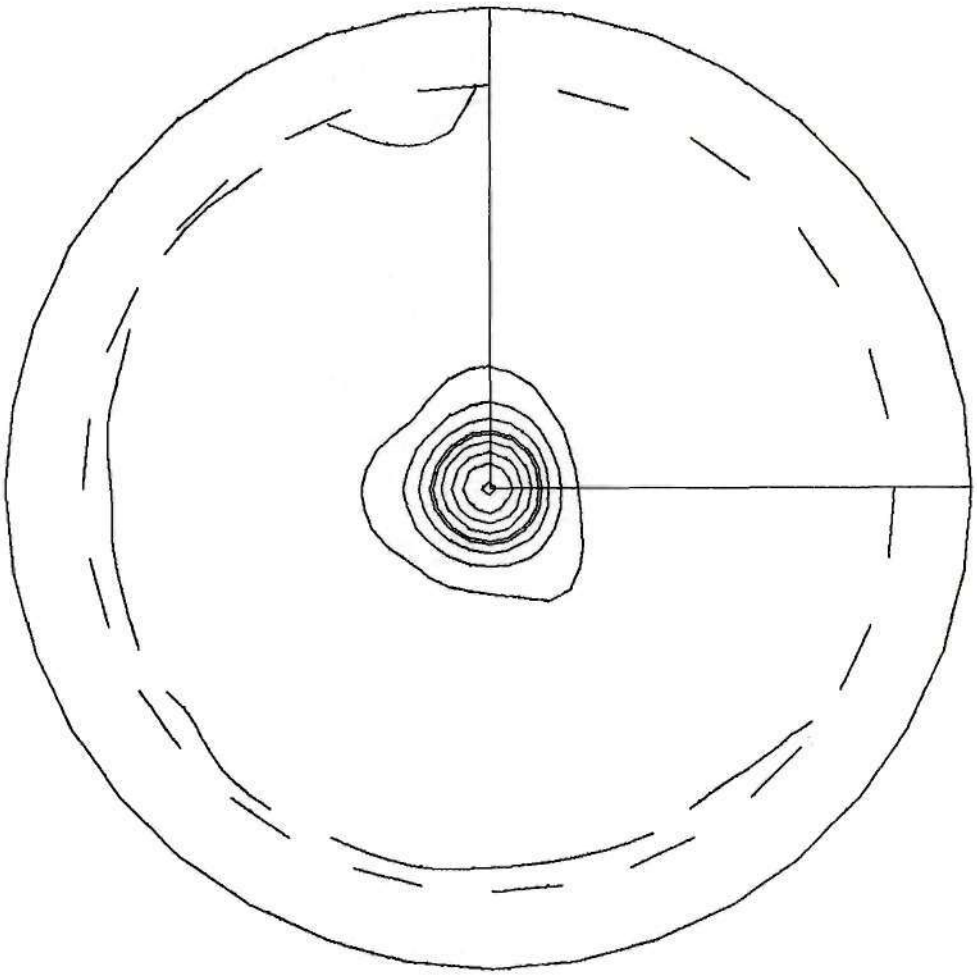

Figure 12. TiC Coating Texture Pole (200)

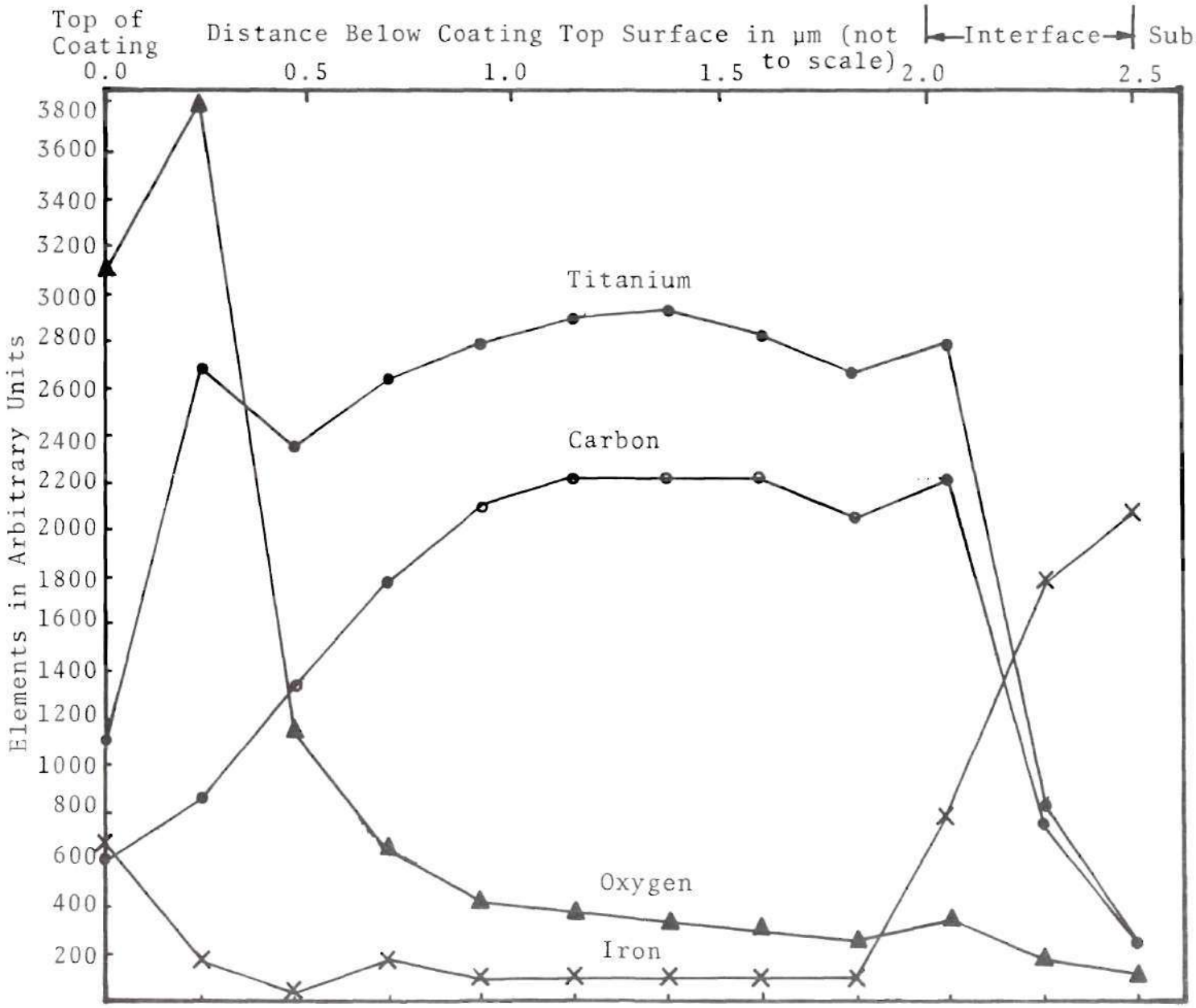

Figure 13. Sputtering Time Vs. Elements in the Coating

Table 2. Auger Electron Spectroscope (AES) Data for the Coating

Sputtering Time Seconds/20	Elements in Arbitrary Units			
	C	Ti	O	Fe
1	605	1097	3093	663
50	860	2679	3814	180
100	1342	2345	1159	43
150	1789	2635	643	170
200	2103	2791	423	95
250	2226	2890	395	108
300	2220	2933	345	90
350	2216	2828	291	87
400	2056	2678	259	108
450	2238	2795	355	786
500	760	844	186	1764
550	254	255	122	2066

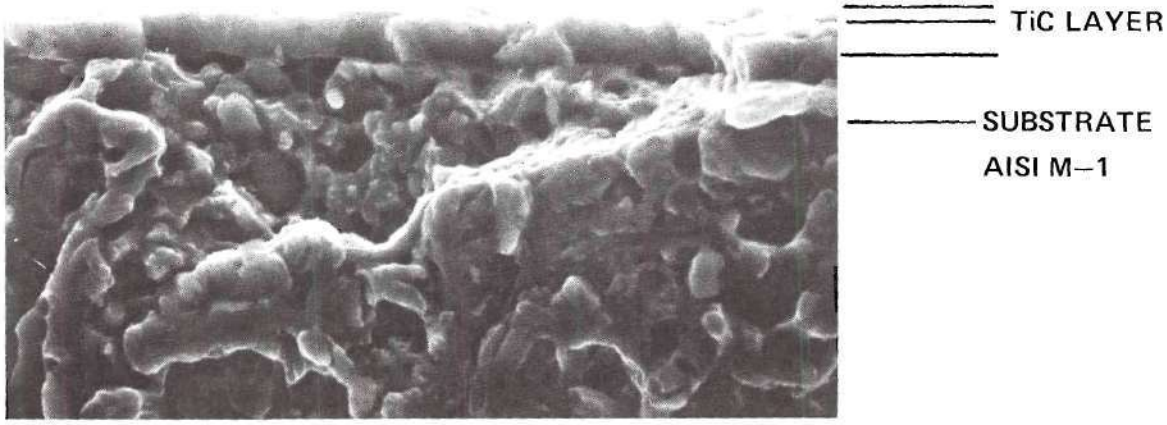

(a) 2400X

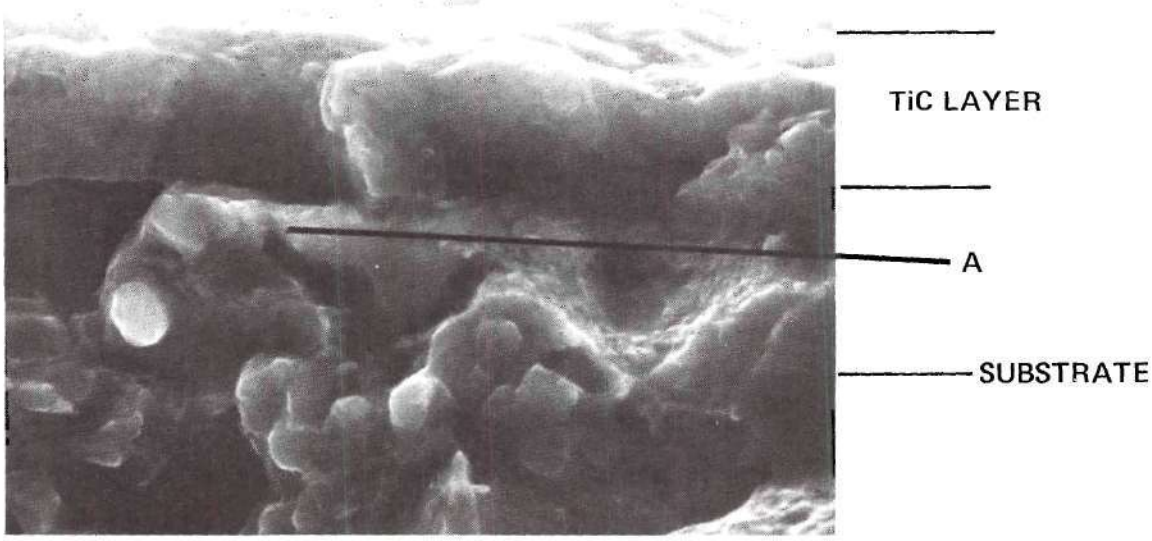

(b) 8000X

Figure 14. Scanning Electron Micrographs of Ion Plated, Heat Treated and Fractured AISI M-1 Tool

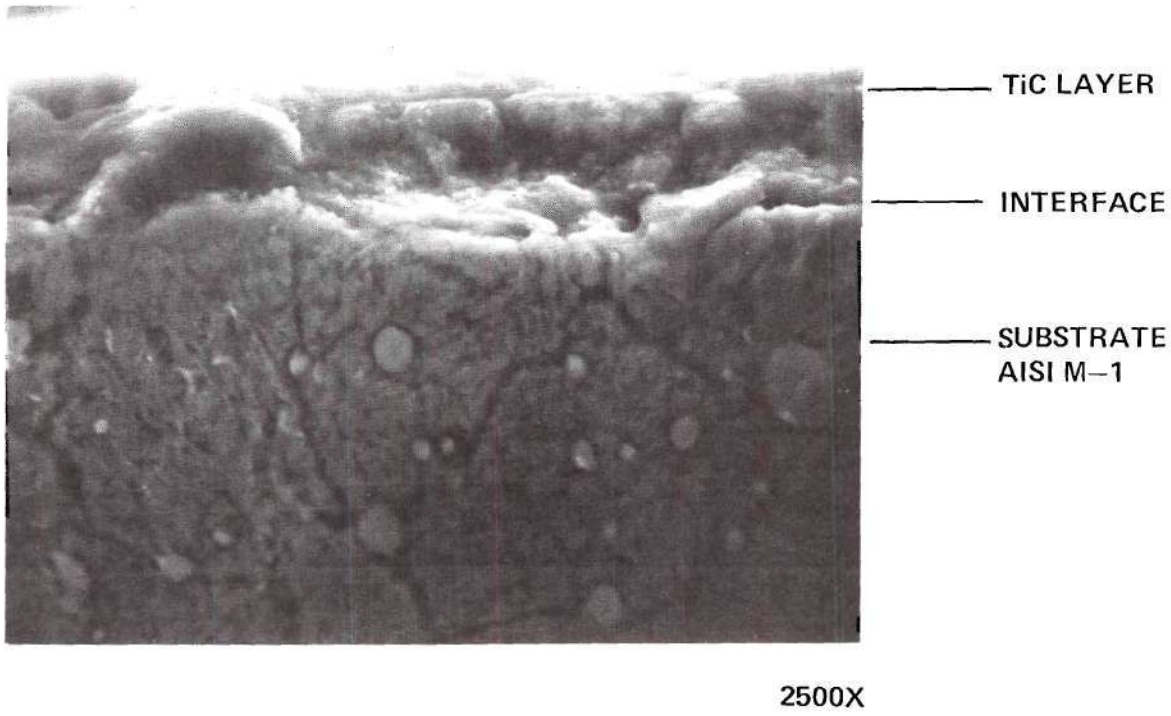

Figure 15. Scanning Electron Photomicrograph of Ion Plated, Heat Treated, Polished and 10% Nital Etched Section of AISI M-1 Tool

was cut from the bar, polished and the hardness profile was taken along the radius and it is shown in Figure 16. Cutting was performed between radii 1.250 inches and 2.250 inches and as seen from Figure 16, the work material is fairly uniform and has an average Brinell hardness of about 188.5 BHN (load = 3000 kg).

Evaluation of the Tool Wear

Machining tests were performed in turning AISI 1045 steel characterized previously with coated as well as uncoated high speed steel inserts. The wear land width was measured after 1, 2, 3, 5, 7.5, 10, 12.5 and 15 minutes of cutting time. The flank wear measurements at the above time intervals are recorded in Tables 4, 5, 6 and 7 for 0 μm, 2 μm, 4 μm and 7 μm thick coated tools respectively at cutting speed 175 ft/min, feed 0.0075 in/rev and depth of cut 0.060 in. No difference in wear measurements was found between the 4 μm thickness and 7 μm thickness coated tools and hence 7 μm thick coated tools were dropped from further testing. This was further confirmed by repeating the test with 7 μm under the same cutting conditions. The wear land width against cutting time in minutes is plotted in Figure 17 under the above cutting conditions of 0 μm, 2 μm and 4 μm thick coated tool inserts. The crater depth measurements are given in Table 8. Crater surfaces of the uncoated and coated (4 μm) tools are shown in Figure 18 as viewed in SEM at 40X.

Table 3. Chemical Analysis of AISI 1045

Element	% Composition
C	0.51
Mn	0.88
P	0.017
S	0.049
Si	0.24
Cu	0.00
Ni	0.00
Cr	0.01
Mo	0.001
Al	0.00
Fe	Balance

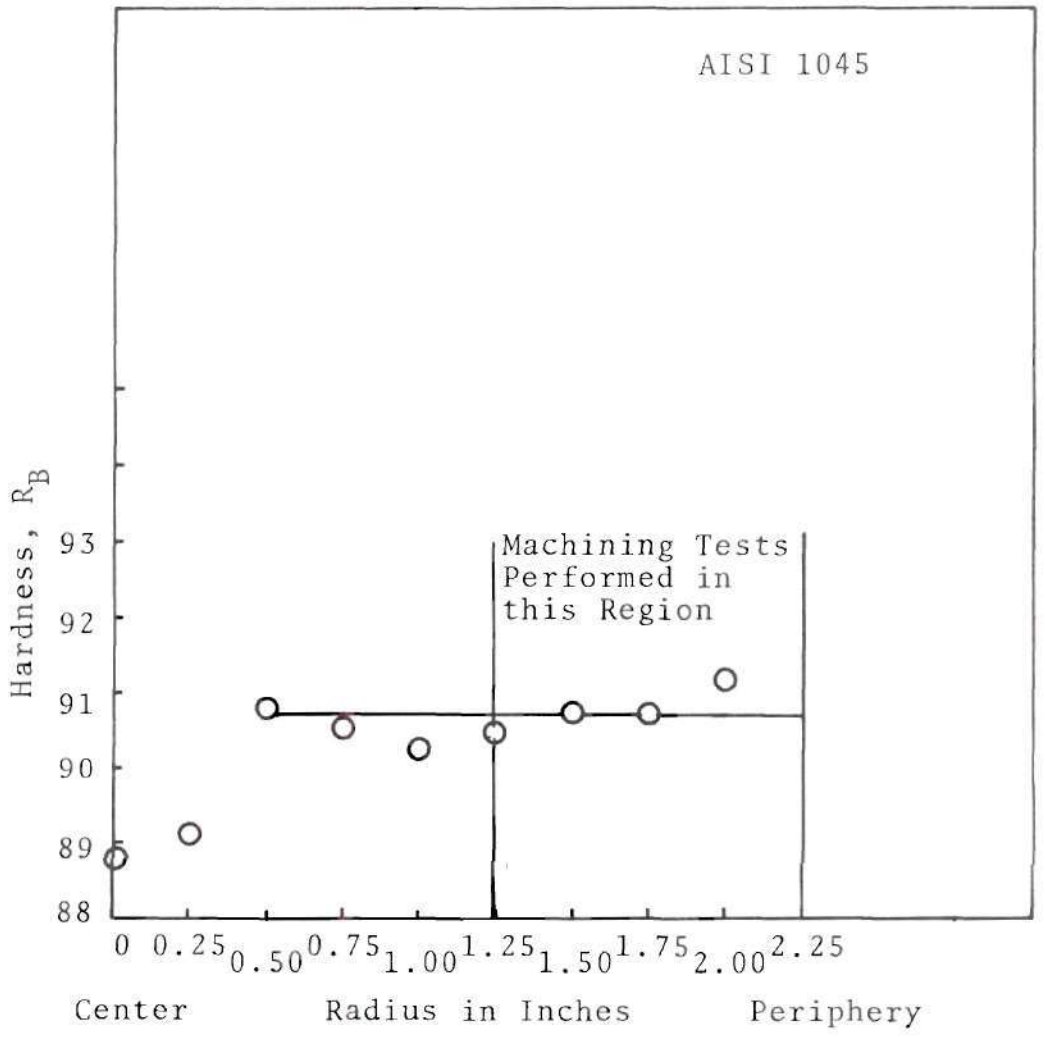

Figure 16. Hardness Profile Along the Radius from the Center of Work Material

Table 4. Flank Wear Data

Date: 11/13/78 Tool: HSS Material: AISI M-1 Coating: 0 μm

Test No.: 9 Work Material: AISI 1045 Hardness: 189 BHN Geometry: 11° Clearance Angle

Continuous/Discontinuous Cutting: Discontinuous

Machining Variables			Wear Land Width		Time
Cutting Speed ft/min	Feed in/rev	Depth of Cut in	Average in x 10^3	Maximum in x 10^3	Minutes
175	0.0075	0.060	could not measure		1
			4.53	5.55	2
			5.21	6.34	3
			5.66	7.70	5
			7.36	9.51	7.5
			8.04	10.20	10.0
			8.61	10.53	12.5
			9.06	11.10	15.0

Table 5. Flank Wear Data

Date: 11/23/78 Tool: HSS Material: AISI M-1 Coating: 2 μm

Test No.: 10 Work Material: AISI 1045 Hardness: 189 BHN Geometry: 11° Clearance Angle

Continuous/Discontinuous Cutting: Discontinuous

Machining Variables			Wear Land Width		Time
Cutting Speed ft/min	Feed in/rev	Depth of Cut in	Average in x 10^3	Maximum in x 10^3	Minutes
175	.0075	.060	--	--	1
			1.00	--	2
			1.18	--	3
			3.33	3.85	5
			3.74	5.44	7.5
			4.42	6.12	10.0
			5.21	7.81	12.5
			6.00	8.83	15.0

Table 6. Flank Wear Data

Date: 11/23/78 Tool: HSS Material: AISI M-1 Coating: 4 μm

Test No.: 8 Work Material: AISI 1045 Hardness: 189 BHN Geometry: 11° Clearance Angle

Continuous/Discontinuous Cutting: Discontinuous

Machining Variables			Wear Land Width		Time
Cutting Speed ft/min	Feed in/rev	Depth of Cut in	Average in x 10^3	Maximum in x 10^3	Minutes
175	.0075	.060	0.68	0.68	1
			0.80	1.470	2
			1.250	1.590	3
			1.69	1.930	5
			2.267	2.830	7.5
			2.600	3.06	10.0
			2.830	4.87	12.5
			3.170	5.66	15.0

Table 7. Flank Wear Data

Date: 11/23/78 Tool: HSS Material: AISI M-1 Coating: 7 μm

Test No.: -- Work Material: AISI 1045 Hardness: 189 BHN Geometry: 11° Clearance Angle

Continuous/Discontinuous Cutting: Discontinuous

Machining Variables			Wear Land Width		
Cutting Speed ft/min	Feed in/rev	Depth of Cut in	Average $in \times 10^3$	Maximum $in \times 10^3$	Time Minutes
175	.0075	.060	.34	.34 coating on flank wiped	1
			.91	.91	2
			1.13	1.36	3
			1.48	1.70	5
			2.270	2.49	7.5
			2.50	3.06	10.0
			3.06	3.10	12.5
			*	*	15.0

*Could not measure because the tool edge was damaged due to an experimental difficulty namely sudden increase in depth of cut on the left near the chuck.

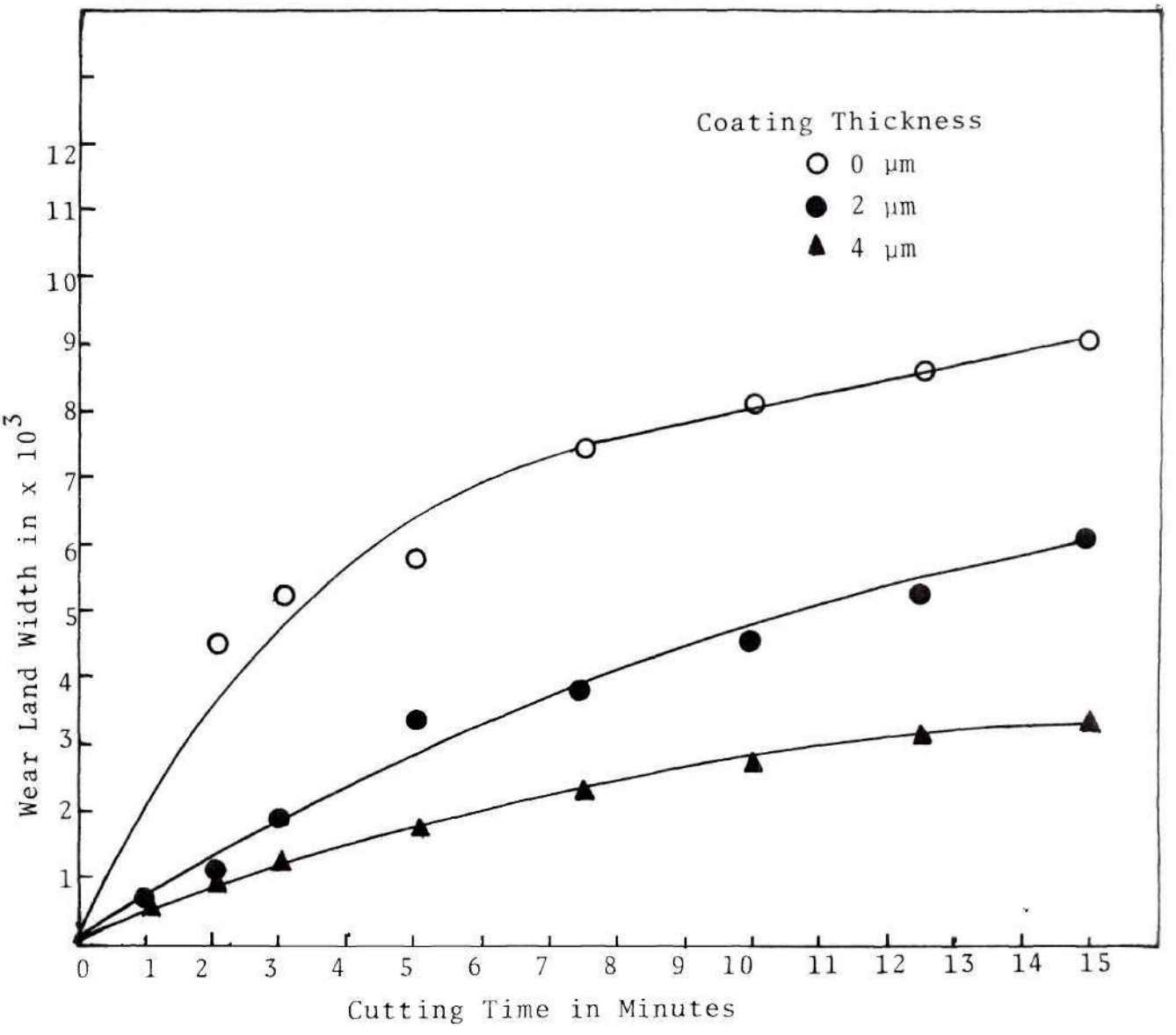

Figure 17. Wear Land Width Vs. Cutting Time at 175 ft/min. Cutting Speed, 0.0075 in/rev Feed and 0.060 in Depth of Cut

Table 8. Crater Depth Measurements for Uncoated, 2 μm Thick Coated and 4 μm Thick Coated AISI M-1 Tools at Cutting Conditions 175 ft/min, .0075 in/rev and 0.060 in.

Tool Coating in μm	Crater Depth in inches	Normalized Crater Depth
0	0.00725	100
2	0.00680	94
4	0.00240	33

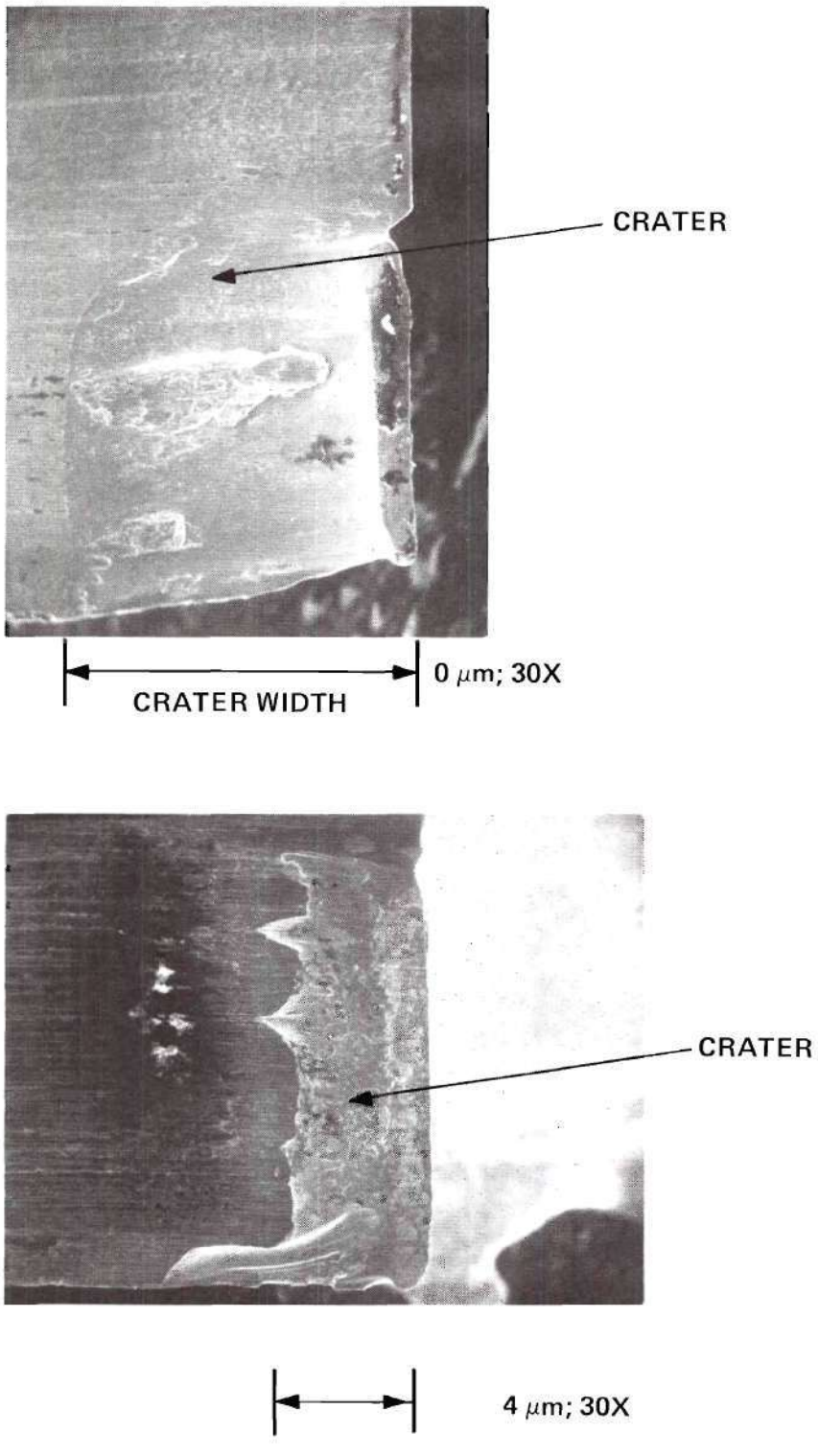

Figure 18. Scanning Electron Micrograph of Uncoated and Coated (4 μm) AISI M-1 Tools after 15 Minutes of Turning at 175 ft/min, 0.0075 in/rev and 0.060 in

Flank wear data under cutting conditions 175 ft/min, 0.0025 in/rev and 0.060 in, are given in Tables 9, 10 and 11 for 0 μm, 2 μm and 4 μm thick coated tools. Wear land width against cutting time is plotted in Figure 19 for the same. The difference from Figure 17 is that the feed is reduced from 0.0075 in/rev to 0.0025 in/rev.

Wear land measurements with cutting time are given in Tables 12 and 13 at 125 ft/min cutting speed, 0.0025 in/rev feed and 0.060 in depth of cut and plotted in Figure 20 for uncoated as well as 4 μm thick coated tools. Table 14 and Figure 21 show the progression of wear with cutting time for 2 μm thick coated tool at cutting speed 150 ft/min, feed 0.005 in/rev and 0.060 in depth of cut. The discussion of these results is presented in the next chapter.

Table 9. Flank Wear Data

Date: 11/25/78 Tool: HSS Material: AISI M-1 Coating: 0 μm

Test No.: 6 Work Material: AISI 1045 Hardness: 189 BHN Geometry: 11° Clearance Angle

Continuous/Discontinuous Cutting: Discontinuous

Machining Variables			Wear Land Width		Time
Cutting Speed ft/min	Feed in/rev	Depth of Cut in	Average in x 10^3	Maximum in x 10^3	Minutes
175	.0025	.060	1.02	1.13	1
			2.40	2.94	2
			2.72	3.28	3
			4.30	5.44	5
			5.44	5.67	7.5
			6.00	6.34	10.0
			6.57	6.80	12.5
			6.91	7.25	15

Table 10. Flank Wear Data

Date: 11/26/78 Tool: HSS Material: AISI M-1 Coating: 2 μm

Test No.: Work Material: AISI 1045 Hardness: 189 BHN Geometry: 11° Clearance Angle

Continuous/Discontinuous Cutting: Discontinuous

Machining Variables			Wear Land Width		Time
Cutting Speed ft/min	Feed in/rev	Depth of Cut in	Average in x 10^3	Maximum in x 10^3	Minutes
175	.0025	.060	0.79	1.02	1
			1.13	1.70	2
			1.25	2.38	3
			2.55	3.00	5
			3.39	4.53	7.5
			4.19	5.44	10.0
			5.50	6.57	12.5
			6.00	6.80	15.0

Table 11. Flank Wear Data

Date: Tool: HSS Material: AISI M-1 Coating: 4 μm

Test No.: 7 Work Material: AISI 1045 Hardness: 189 BHN Geometry: 11° Clearance Angle

Continuous/Discontinuous Cutting: Discontinuous

Machining Variables			Wear Land Width		Time
Cutting Speed ft/min	Feed in/rev	Depth of Cut in	Average in x 10^3	Maximum in x 10^3	Minutes
175	.0025	.060	0.51	0.91	1
			0.79	1.47	2
			1.08	1.53	3
			1.47	1.81	5
			1.93	2.72	7.5
			2.21	2.78	10
			2.61	3.00	12.5
			2.89	3.63	15

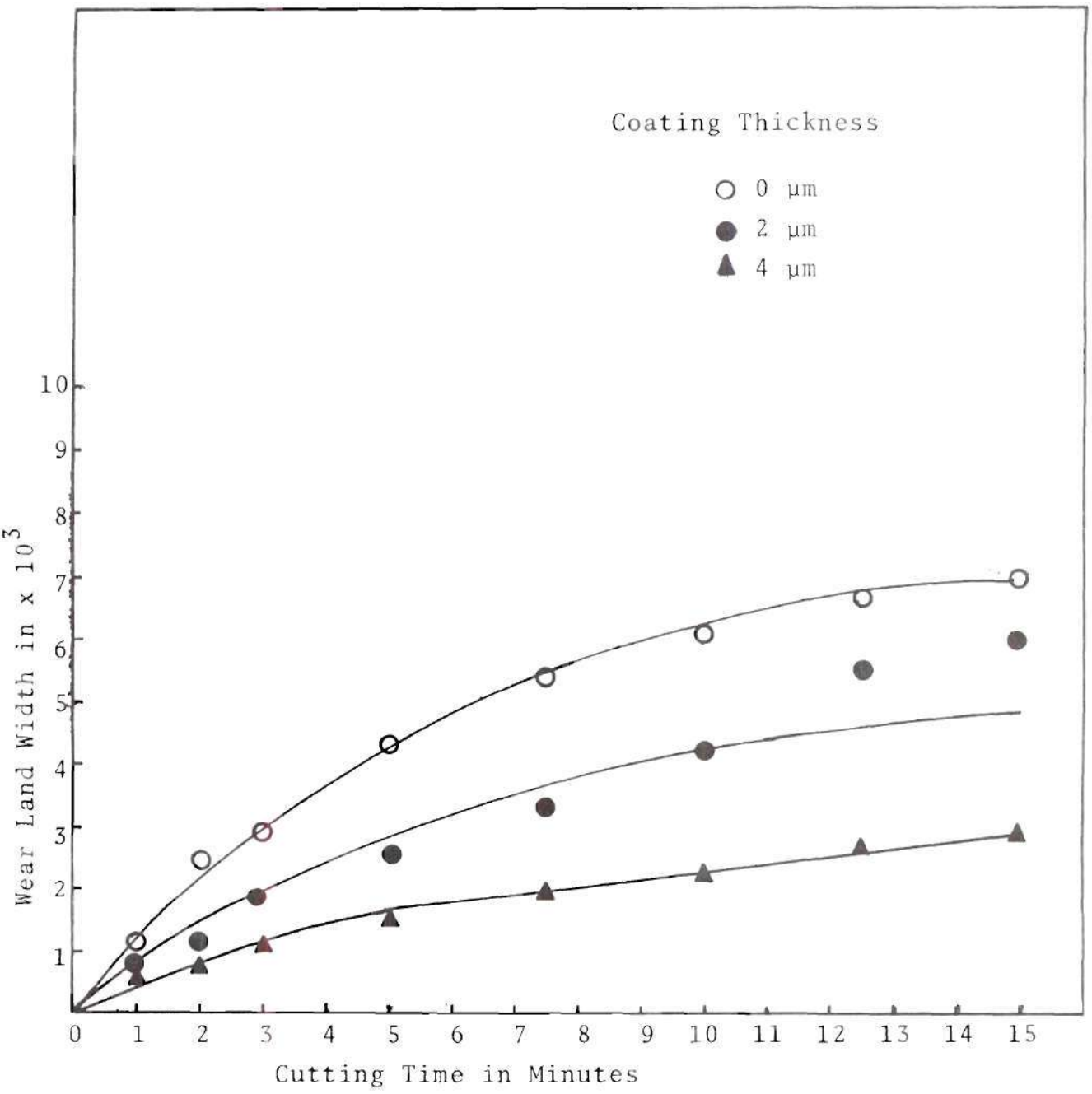

Figure 19. Wear Land Width Vs. Cutting Time at 175 ft/min Cutting Speed, 0.0025 in/rev Feed, and 0.060 in Depth of Cut

Table 12. Flank Wear Data

Date: 11/26/78 Tool: HSS Material: AISI M-1 Coating: 0 μm

Test No.: 2 Work Material: AISI 1045 Hardness: 189 BHN Geometry: 11° Clearance Angle

Continuous/Discontinuous Cutting: Discontinuous

Machining Variables			Wear Land Width		Time
Cutting Speed ft/min	Feed in/rev	Depth of Cut in	Average in x 10^3	Maximum in x 10^3	Minutes
125	.0025	.060	0.91	1.02	1
			1.81	2.00	2
			2.49	3.05	3
			3.40	3.74	5
			4.53	4.53	7.5
			5.44	5.44	10.0
			5.72	5.72	12.5
			5.89	5.89	15.0

Table 13. Flank Wear Data

Date: 11/26/78 Tool: HSS Material: AISI M-1 Coating: 4 μm

Test No.: 3 Work Material: AISI 1045 Hardness: 189 BHN Geometry: 11° Clearance Angle

Continuous/Discontinuous Cutting: Discontinuous

Machining Variables			Wear Land Width		Time
Cutting Speed ft/min	Feed in/rev	Depth of Cut in	Average in x 10^3	Maximum in x 10^3	Minutes
125	.0025	.060	0.453	0.453	1
			0.793	0.793	2
			1.13	1.530	3
			1.47	1.530	5
			1.70	1.70	7.5
			1.93	1.93	10
			2.21	2.21	12.5
			2.32	2.32	15.0

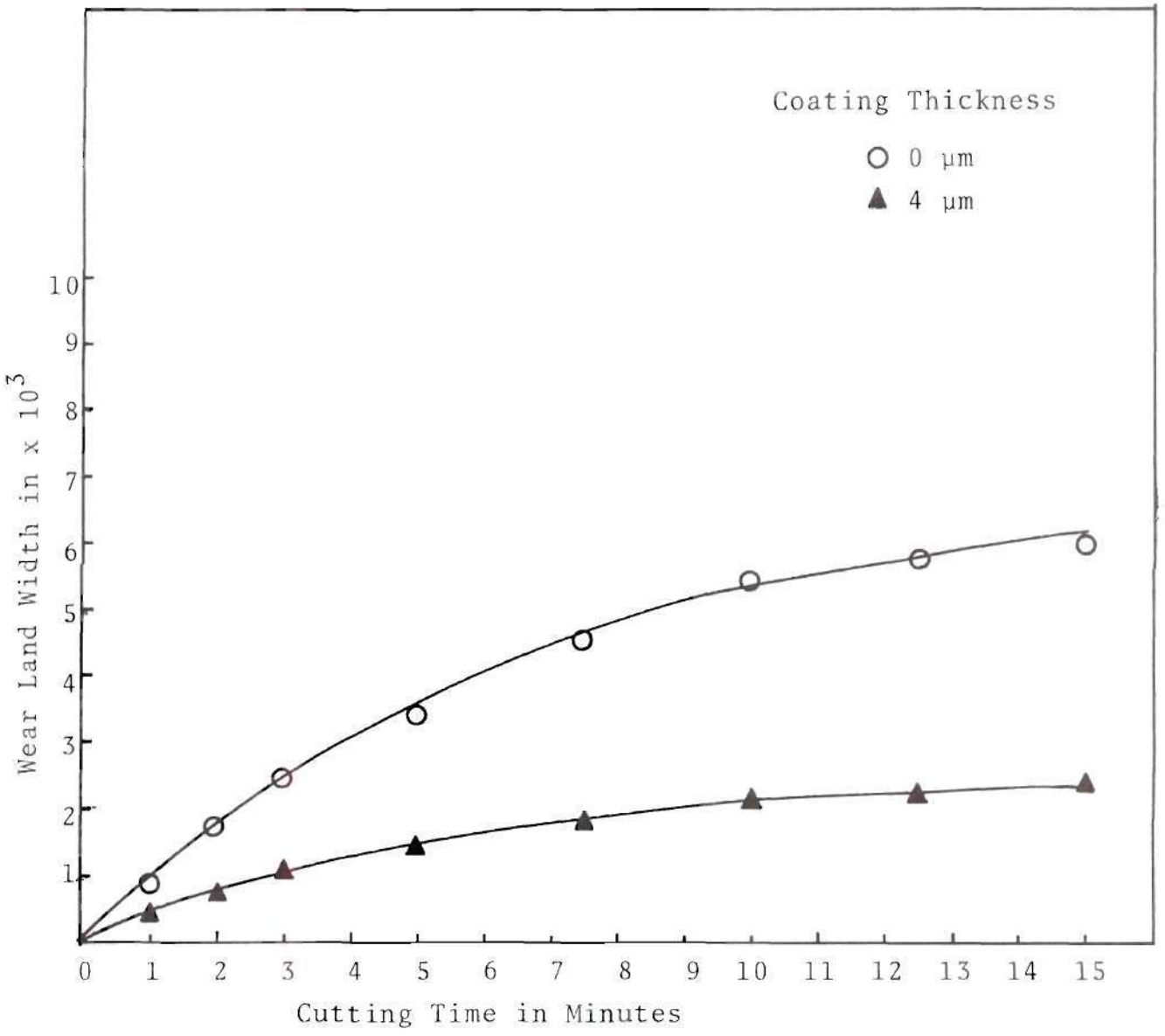

Figure 20. Wear Land Width Vs. Cutting Time at 125 ft/min Cutting Speed, 0.0025 in/rev Feed and 0.060 in Depth of Cut

Table 14. Flank Wear Data

Date: 11/24/78 Tool: HSS Material: AISI M-1 Coating: 2 μm

Test No.: 1 Work Material: AISI 1045 Hardness: 189 BHN Geometry: 11° Clearance Angle

Continuous/Discontinuous Cutting: Discontinuous

Machining Variables			Wear Land Width		Time
Cutting Speed ft/min	Feed in/rev	Depth of Cut in	Average in x 10^3	Maximum in x 10^3	Minutes
150	.005	.060	0.57	0.79	1
			0.79	0.91	2
			0.91	1.13	3
			1.13	1.47	5
			1.59	2.04	7.5
			1.93	2.44	10.0
			2.38	3.28	12.5
			4.10	4.75	15.0

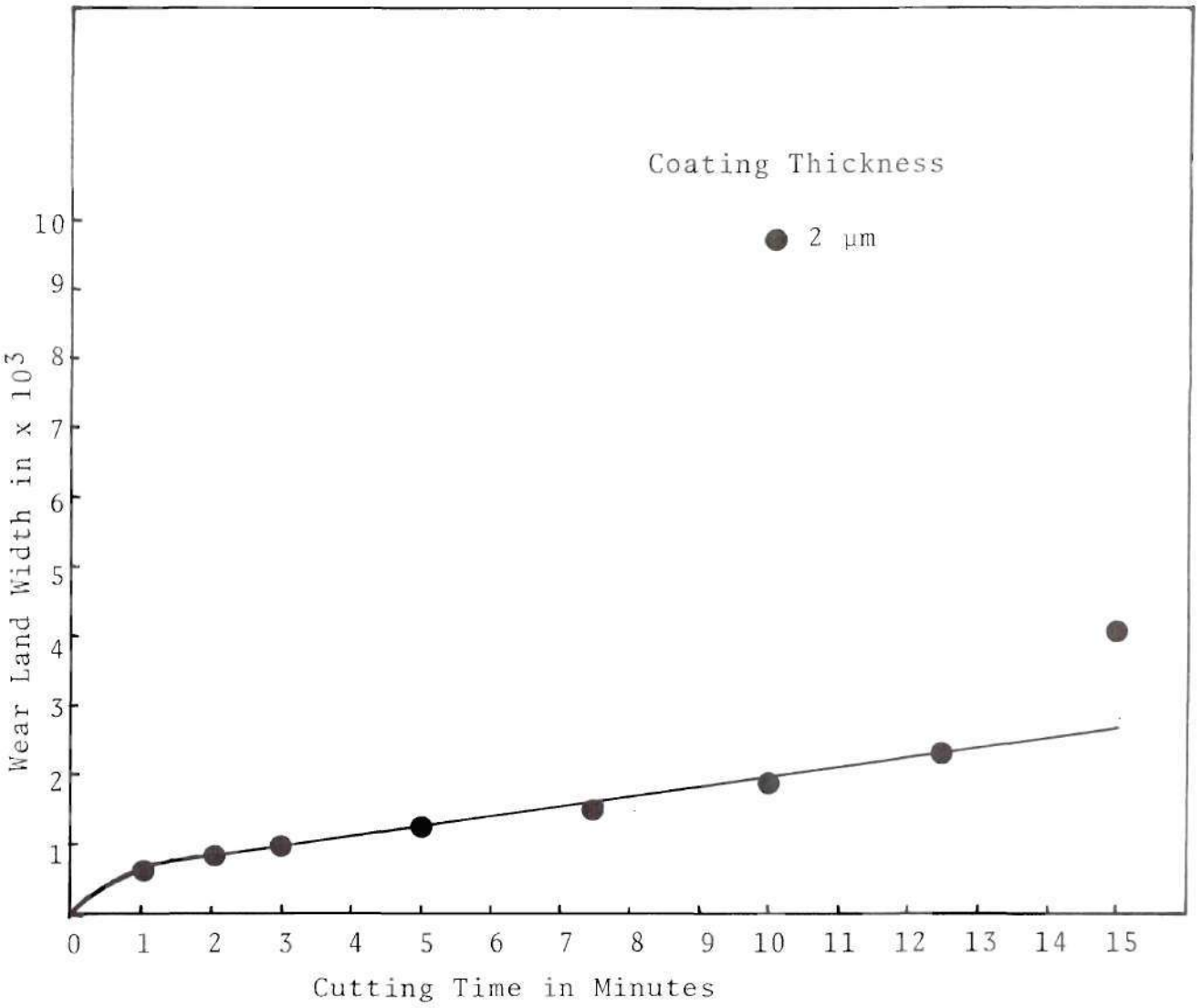

Figure 21. Wear Land Width Vs. Cutting Time at 150 ft/min Cutting Speed, 0.005 in/rev Feed and 0.060 in Depth of Cut

CHAPTER V

DISCUSSION OF RESULTS

Prehardened and ground high speed steel tools were ion plated with titanium and heat treated to obtain titanium carbide and the TiC thus obtained was identified with X-ray diffraction and the stoichiometry was checked with the Electron Probe Micro Analyzer (EPMA). The coating composition variation with coating depth was also obtained by analyzing the Auger electrons. The coated tool was fractured and the fractured surface was examined in the Scanning Electron Microscope (SEM) and the coating was found to be adherent. The tools were then evaluated for improvement against wear. The resulting improvements in tool wear as a result of this technique, appear to be due to the superior adhesion of the coating to the substrate, the composition profiles developed and the near perfect stoichiometry of the titanium carbide contributing in concert with each other. These effects are systematically discussed in the following sections.

Preparation of the Coating

Prior to coating the AISI M-1 high speed steel inserts were ground flat. It will also be recalled that the tool inserts were then cleaned in acetone and made ready for ion plating.

Ion plating involves two steps; namely sputter cleaning and ion plating. The tool inserts were also sputter cleaned for 15 minutes with 2.9 kV and 100 mA applied to the substrate. During sputter cleaning, ionized argon atoms or molecules bombard the surface of the tools and thus remove surface atoms by momentum transfer. First the adsorbed as well as chemisorbed atoms are removed and then the surface atoms of the tool substrate are removed. The sputter cleaned surface has peaks and valleys on an atomic level and thus the surface is ready to receive the titanium plating.

The system was then changed to ion plating mode and the filament was turned on. The ion plating was carried out at 1.4 kV and 150 mA for about 3 minutes. A DC coil with potential difference of 34V, a current of 2.2 amperes and approximately 600 coil turns was surrounding the bell-jar near the substrate. For a coil diameter of 20 in, the magnetic field strength produced at the center of the bell-jar is approximately 33 Gauss. This magnetic field increases the ionization of the gas in the bell-jar, resulting in a dense plasma. This in turn will increase the ionization probability of titanium atoms.

In ion plating, the titanium filament was thermally evaporated in argon plasma. Thermally evaporated titanium atoms have energies in the range of about 0.1 eV and a mean value for the energy involved is given by $\frac{3}{2}$ kT, where k is Boltzmann Constant, 0.861×10^{-4} eV/atom K and T is evaporation

temperature of titanium at a pressure of 20 microns, 2412 K. Therefore $\frac{3}{2}$ kT represents about 0.3 eV per titanium atom.

When the electrons collide with neutral atoms of the argon sputtering gas, ions or excited atoms are formed. The energy required to raise argon gas atom from the ground state to the lowest excited state is 11.55 eV[100]. The ionization potential of titanium is only 6.78 eV, which is far less than the ionization potential of the argon. Hence it is possible for the excited argon atom or molecule to collide with the evaporated titanium atom to produce a titanium ion. Recent estimates have been made of the relative contribution to substrate bombardment by ions (10%) and energetic neutrals (90%) in ion plating.[61,62] Even for those titanium ions, the energy attained in the field is in the range of a few keV and any implantation of titanium ions is unlikely. Ion implantation requires energies in the range of several hundred keV.[102] However, simultaneous sputtering and plating may well have caused embedding of titanium ions in the cleaned surface layers of the high speed steel tool matrix. This enhances the adhesion of the deposit to the substrate.

Post Heat Treatment of the Tools

The tools plated with titanium were subsequently austenitized in vacuum at 1200 C for five minutes and then quenched in argon. After quenching, hardened high speed steel consists of tempered martensite, undissolved carbides

and retained austenite. The carbides present in the high speed steel are usually chromium-rich carbide $M_{23}C_6$, molybdenum-tungsten-rich carbide M_6C and vanadium-rich carbide M_4C_3[4]. During austenitization, when ferrite is transformed into austenite, $M_{23}C_6$ type carbide goes into solution first, complete solution occurs at about 1100 C. At 1200 C small amounts of M_6C and M_4C_3 type carbides go into solution. The high austenitizing temperature of 1200 C is required to enrich the austenite in carbon so as to achieve enough hardness of the martensite matrix when quenched.

During the austenization treatment at 1200 C of the coated specimens, the conditions are suitable for diffusion of carbon from the carbon rich austenite into the titanium layer to form titanium carbide. Thermodynamics of titanium carbide formation is discussed in the following sections.

The chemical reaction between solid titanium and solid carbon is written,

$$Ti(solid) + C(solid) = TiC(solid).$$

The Gibbs free energy change for the reaction is written,

$$\Delta G_T = \Delta H_T - T\Delta S_T.$$

When expressed in terms of standard Gibbs free energy, ΔG_T°, which can be calculated from tabulated ΔH_T° and ΔS_T° values,

$$\Delta G_T - \Delta G_T^\circ = RT \ln \frac{a_{TiC}}{a_{Ti} a_C}$$

where a's are activities for the reaction components and for this case are given below.

a_{TiC} could be less than 1 say 0.5 because of variable stoichiometry

a_{Ti} is taken as 1.0 for the case of pure titanium on the steel substrate, and

a_C = 0.2 (as taken from Gaskell[113] on a discussion of a_C in austenite for a carbon concentration of 0.44).

Using tabulated standard thermodynamic quantities,

$$\Delta G_T = -40,890 + RT \ln \frac{0.5}{1(0.2)}$$

$$= -40,890 + (1.987)(1473)(0.916)$$

$$= -40,890 + 2682$$

$$= -30,208 \text{ Cal/mol.}$$

Thus the reaction can be expected to proceed to the right for the spontaneous production of TiC.

The formation of titanium carbide is possible only if the carbon is available to react with titanium. The source

for carbon is the high speed steel substrate and in particular the carbon rich austenite at 1200 C. Austenite matrix contains about 0.44% C by weight at 1200 C. In the case of 2 μm thick layer, for every titanium atom in the coating there are about 49 carbon atoms in the austenite matrix of 0.125 in x 0.500 in x 0.500 in high speed steel substrate (the calculation is presented in Appendix F). Therefore the substrate has adequate amount of carbon to supply to react with titanium.

The carbon in the substrate has to travel to the surface layer through austenite and then through titanium to react with titanium. The process by which carbon travels is diffusion. At 1200C, diffusion coefficient of carbon in austenite is 2×10^{-6} cm^2/sec where as the diffusion coefficient of carbon in titanium is 2.78×10^{-8} cm^2/sec[98]. At zero time, there is very little or no carbon diffusing. For a period of five minutes, the mean penetration distance ($\bar{x}$) which is a measure of the distance over which an appreciable amount of diffusion has occurred is calculated according to $\bar{x} = \sqrt{Dt}$. $\bar{x}$ for carbon in FCC iron is 24.5×10^{-3} cm and $\bar{x}$ for carbon in titanium is 28.9×10^{-4} cm. That means the distance over which appreciable diffusion occurs is 10 times more for carbon in FCC iron than for carbon in titanium. This is an upperbound value because the effect of different alloying elements on the diffusion rate is neglected. Even if the diffusion rate of carbon is slowed by a factor of 10,

there will be enough carbon delivered to cope with the diffusion of carbon through titanium. Therefore, the rate limiting factor is the diffusion of carbon through titanium.

From the estimations above, it is evident that the reaction to form titanium carbide is thermodynamically favorable, there is enough carbon in the substrate matrix to satisfy titanium in the coating and the conditions are suitable for carbon to be delivered to titanium by diffusion.

Because of various diffusion processes, there will be composition gradients present. The region over which the composition gradients exist is estimated to be about half a micrometer, straddling the interface as will be seen from the Auger Electron Spectroscopy result (Figure 13). This effect is confirmed partly by the appearance of the fractured tool as shown in Figure 14 and the etched section of the coated tool as shown in Figure 15, where it may be seen that fracture process did not seek out the interface.

Chemistry and Structure of the Coating

The conditions prevailing in the current experiment are thermodynamically favorable for titanium and carbon at 1200 C to form titanium carbide as illustrated in the previous section. This fact has been verified by X-ray diffraction. At the same time, the stoichiometry of the coating varied from $TiC_{0.93}$ at the center to $TiC_{0.88}$ at the corner of the tool as determined by an EPMA. At this juncture it should be

established that it is not uncommon to use electron microprobe for measuring the stoichiometry of thin films:[69,106] for example Hickmott and Baglin[69] used electron microprobe and helium ion back scattering to measure the stoichiometry of RF-sputtered SiO_2 films with good agreement and at a precision of ≤1%. The electron accelerating voltage was 10 kV: the penetration depth for such electrons, reported by Hickmott and Baglin, was 1 μm, about half the thickness of the sputtered films used. Thus the variation in stoichiometry from the center to the corner of the tool revealed by EPMA is probably real. This variation may occur in the following way. Carbon diffuses from the substrate matrix into the titanium and reacts to form titanium carbide. At the center of the tool the substrate is about 0.125 inch thick whereas at the corner of the tool the substrate material is physically undercut and this could well be associated with a local diminishment in carbon thus resulting in somewhat carbon deficient TiC. Consequently the titanium carbide near the corner or the cutting edge is deficient in carbon.

The variation in stoichiometry and deficiency of carbon in titanium carbide coating could be eliminated by depositing titanium in a reactive atmosphere such as methane gas. Of course, then the deposition rate will be lower.

It is interesting to note that there is also oxygen present on the surface as is evident from Figure 13. The surface oxidation might have occurred due to the gettering

effect of titanium with traces of oxygen occurring probably during heat treatment. The X-ray diffraction data shows only titanium carbide and titanium oxide but no other compounds. Hence there is no reason to believe that there are any ternary compounds formed on the tool surface. Furthermore no nitrides were observed.

After treatment it will be recalled that the tools were agitated ultrasonically in alcohol for several minutes and the coating was observed to be adherent. A peel test with an adhesive tape also demonstrates that the coating has good adherence to the substrate.

Preferred Orientation of the Coating

Vapor deposited films are well known to have varying amounts of preferred orientations in them. The X-ray diffraction pattern of the as-coated tool (shown in Figure B-1 in Appendix B) reveals that the coating is titanium with a strong texture in the basal plane (002) and this is in agreement with the basal plane texture observed by Turk and Marcus[104] in the case of physical vapor deposited titanium. The tool with the titanium coating is of course, then heat treated to convert titanium to titanium carbide. The titanium carbide thus formed has a strong preferred orientation with the cube faces developing from the basal planes in close packed hexagonal titanium as will be seen from Figure 10.

Raghuram and Bunshah[49] report that considerable amounts

of preferred orientation exist in (220) plane at substrate temperatures below 830 C in the case of TiC deposits made by Activated Reactive Evaporation. As the temperature, at which deposition takes place, was increased, the titanium carbide in the deposit tended to take up more random orientation.

Mah, Nordin and Fuller[37] used a triode sputtering process to deposit TiC on tungsten carbide cutting tools. They report a preferred orientation of (111) and fine columnar grain structure. Greene and Pestes[19] did not report any information on the texture of sputtered TiC on steel.

In the present investigation, the transformation of titanium (in the coating) and the carbon (diffusing from the substrate) to titanium carbide occurs during heat treatment process (1200 C). The apparent texture is due to the basal plane preferred orientation established by the coating process prior to heat treatment, because of deposition at a relatively lower temperature. Evidently the post heat treatment was unable to randomize the orientation of the titanium carbide formed during heat treatment.

Gilman and Roberts,[103] while studying TiC and TiB_2 single crystals to determine elastic constants, observed that TiC cleaves along (100) planes. They attribute this cleavage to the minimum value of surface energy (2500 erg/cm^2) for (100) planes in the case of TiC.

The fiber texture observed in (002) plane may not offer much resistance to cleavage in the present investigation.

Ion plating in a reactive atmosphere might result textures similar to the observation of Bunshah and Raghuram.[49]

Performance of the Tools

The results obtained from the machining tests, performed, are presented in the last chapter. Flank wear measurement was used as the performance index of the tool. The progression of wear land width with cutting time in minutes is shown in Figures 17, 19, 20, and 21 under various cutting conditions using coated and uncoated tools. It is observed from these figures that the flank wear of TiC coated tools is much less than that of the uncoated tools under the same cutting conditions.

In a typical machining situation, at a cutting speed of 175 ft/min, a feed of 0.0075 in/rev and a depth of cut of 0.060 in, at the end of 15 minutes of elapsed cutting, a tool coated with 4 μm thick coating exhibited only about 35% of the wear land width of an uncoated tool. In another machining test, at a cutting speed of 125 ft/min, a feed of 0.0025 in/rev and a depth of cut of 0.060 in, 4 μm thick TiC coated tool showed only 39% of the wear land width of the uncoated tool. In a third case, at a cutting speed of 175 ft/min, a feed of 0.0025 in/rev and a depth of cut of 0.060 in, the 4 μm thick TiC coated tool exhibited only about 42% of the flank wear of the uncoated tool, at the end of fifteen minutes of cutting.

The three situations, cited above, demonstrate that the flank wear is reduced by about 60% by coating with 4 μm thick TiC layer on high speed steel. In the absence of rigorous statistical analysis, the above numbers represent the mean values only since the scatter is not presented. Because of experimental difficulties, associated with the machine tool neither the performance of the experiment at all the design conditions nor the repetition of the experiment was possible. However, the graphical results indicate the diverging nature of the flank wear curves to demonstrate that the TiC coated high speed steel is in fact superior to uncoated tool in reducing flank wear.

The improved performance of the coated tools probably is due both to the superior wear resistance of the titanium carbide and the adhesion of the coating to the substrate. The adhesion can be attributed to the ion plating and post heat treatment process. The diffusion of the titanium into the substrate is, of course, one of the principal reasons for the good adhesion characteristics evidenced.

Limited crater wear measurements partly support the tool wear improvement observed in flank wear measurements. Crater depth on a 4 μm thick coated tool was only 33% of that on the uncoated at the end of 15 minutes of cutting, at a cutting speed of 175 ft/min, a feed of 0.0075 in/rev and a depth of cut of 0.060 in. In other words, the crater in the case of an uncoated tool is 3 times as deep as the one on the

4 μm thick coated tool. The existence of crater on the TiC coated high speed steel may be due to the hardness of the substrate.

In a recent review of metal cutting from a materials viewpoint, Doyle and Samuels[93] point out that the high temperature (of the order of 1000 C) generated in the secondary shear zone, which causes overtempering of the secondary carbides, has a major influence on tool wear. Doyle[94] studied systematically the effect of different heat treatments on the wear of high speed steel (AISI M-2) cutting tools in turning a 0.46% C plain carbon steel under dry cutting conditions of 100 ft/min, 0.010 in/rev and depth of cut of 0.100 in. He observed crater wear in the case of double-tempered and triple-tempered tools after five minutes of cutting whereas no crater was evident on the as-quenched and single-tempered tool tips. However the converse of this situation was found for flank wear. The authors did not give a reason but retained austenite may be the reason. Therefore, the substrate hardness is extremely important in the case of crater wear.

In the present study, the substrate hardness was measured prior to testing for tool wear. The hardness on the Rockwell C scale was $64 \pm \begin{smallmatrix}.9\\.8\end{smallmatrix}$. This is not in the range of maximum attainable hardness (Rc 65-66). The lower hardness may be due to a partial carbon deficiency in the substrate.

As is evident from the powder diffraction pattern of

the coating after heat treatment, there exists a small amount of titanium oxide. Hence it appears that all the titanium deposited is not converted to titanium carbide. The TiC formed however appears to have good stoichiometry. The lower substrate hardness might explain the reason for the existence of crater on the TiC coated high speed steel tool. Choice of better substrate materials should obviously be explored in further work.

CHAPTER VI

CONCLUSIONS AND RECOMMENDATIONS

Ion plating as used in this study does clearly require post heat treatment to convert titanium to titanium carbide. Bunshah et al.[23,24,54] used ion beam melting of the target and substrate heating in Activated Reactive Evaporation process to obtain refractory compounds. The heat treatment of the ion plated tools evidenced here not only helps the formation of titanium carbide but also enhances the diffusion of the elements into and out of the substrate. The coating formed, after ion plating and heat treatment, is titanium carbide as confirmed by X-ray diffraction.

The coating does not terminate abruptly at the interface between the coating and the substrate but there is an interfacial layer of about half a micrometer (μm) for a 2 μm thick coating on the tool. This interfacial layer may be in part responsible for the adhesion of the coating. This interfacial layer cannot be attributed to the ion plating process alone but it is undoubtedly due to the combination of ion plating and heat treatment of the plated tools.

The stoichiometry of the titanium carbide formed varied from $TiC_{0.88}$ at the corner of the tool insert to $TiC_{0.93}$ at the center of the tool insert. In the case of the

coated carbide tools their superior machining performance has been attributed substantially to the near perfect stoichiometry of the carbide coating achieved by Chemical Vapor Deposition. The closer the carbide proceeds to perfect stoichiometry, the higher will be the hardness of the carbide, because of the larger number of bonds involved. Hence the stoichiometry of the titanium carbide obtained by ion plating and post heat treatment is a major factor in the improvement of the cutting performance of the coated high speed steel inserts. The coating appears to have some preferred orientation, even though the mobility of the atoms was permitted by the post heat treatment process.

Tool wear tests, conducted in turning hot rolled silicon killed fine grain special quality AISI 1045 steel with coated as well as uncoated tools, demonstrate that the coated tools are superior to uncoated tools. In a typical cutting situation at 175 ft/min cutting speed, 0.0075 in/rev feed and 0.060 in depth of cut, at the end of 15 minutes of cutting the 2 μm thick coated tool showed about 67% of the uncoated tool wear land width and the 4 μm thick coated tool showed only about 35% of the uncoated tool wear land width. Crater wear measurements at the same cutting condition indicate that the crater formed on the 4 μm thick coated tool at the end of 15 minutes is only 33% as deep as it is on the uncoated tool. In other words, the crater in the case of uncoated tool is 3 times as deep as the one on the 4 μm

thick coated tool.

The coating thickness does appear to influence the coating in reducing tool wear and thus increases the effective tool life. Coating thicknesses which have been tested are 2 μm, 4 μm and 7 μm. The 4 μm thickness of the coating appears to improve resistance against wear appreciably and this is in agreement with the results of Su and Cook[20] and Bunshah et al.[23,24]

It can therefore be concluded that the titanium carbide coating obtained by ion plating and post heat treatment reduces the tool wear under the same cutting conditions by a factor of three when compared to an uncoated tool. As far as the drawbacks are concerned, the post heat treatment appears to pose problems in the case of complex tools.

Regarding recommendations for future research work, field assisted sputtering, chemical vapor deposition along with post heat treatment and ion implantation appear to be promising potential techniques for obtaining refractory compounds on high speed steel tools. Work on the first two methods is already in progress. Ion implantation still is in its infancy as far as cutting tool applications are concerned because of the expense and the deposition rate.

Referring to some recent developments in this context, Pierson[44] investigated the feasibility of using chemical vapor deposition to deposit TiCN at low temperature and found that substrate temperature of at least 600 C is

needed to obtain a satisfactory coating. The heating of the substrate is not desirable in the case of high speed steel unless it is heat treated afterwards. Carson et al.[38] believe that the wear resistance of a carbide during high speed cutting is inversely proportional to the free energy of formation of the carbide; the lower the free energy of formation, the greater the wear resistance of the coating. The free energies of formation of nitrocarbides and oxynitrocarbides of titanium are lower than the free energy of formation of TiC and these carbides/oxides/nitrides of titanium could be applied to a variety of surfaces including high speed steel tools to form a hard protective layer.

Thus it may be feasible to deposit highly wear resistant carbides, nitrides, carbonitrides and boronitrides of titanium on high speed steel either by field assisted reactive sputtering or by chemical vapor deposition and post heat treatment of the high speed steel.

APPENDICES

APPENDIX A

STOICHIOMETRY OF TITANIUM CARBIDE COATING

The weight fraction is obtained as titanium 81.19% and carbon 18.81% at the center of the insert. The atomic fraction is calculated as follows:

The atomic weight of titanium is 47.9 and the atomic weight of carbon is 12.011. The number of titanium atoms in 81.19 gms of titanium are 81.19/47.9 (6.02×10^{23}) i.e. $1.69 \times (6.62 \times 10^{23})$ atoms. The number of carbon atoms in 18.81 gms of carbon are 18.81/12.011 (6.02×10^{23}) i.e. $1.59 (6.02 \times 10^{23})$ atoms. The total number of atoms in 100 gms of the alloy are $3.26 (6.02 \times 10^{23})$. The atomic fraction of Ti is 0.52 and the atomic fraction of carbon is 0.48. Hence the titanium carbide at the center has a composition of $TiC_{0.93}$. Similar calculations show that the titanium carbide at the corner is $TiC_{0.88}$.

APPENDIX B

POWDER DIFFRACTION PATTERN OF AS-COATED AISI M-1 TOOL

The attached Figure B-1 shows the powder diffraction pattern of the as-coated AISI-M-1 tool. The diffraction pattern indicates the coating is titanium.

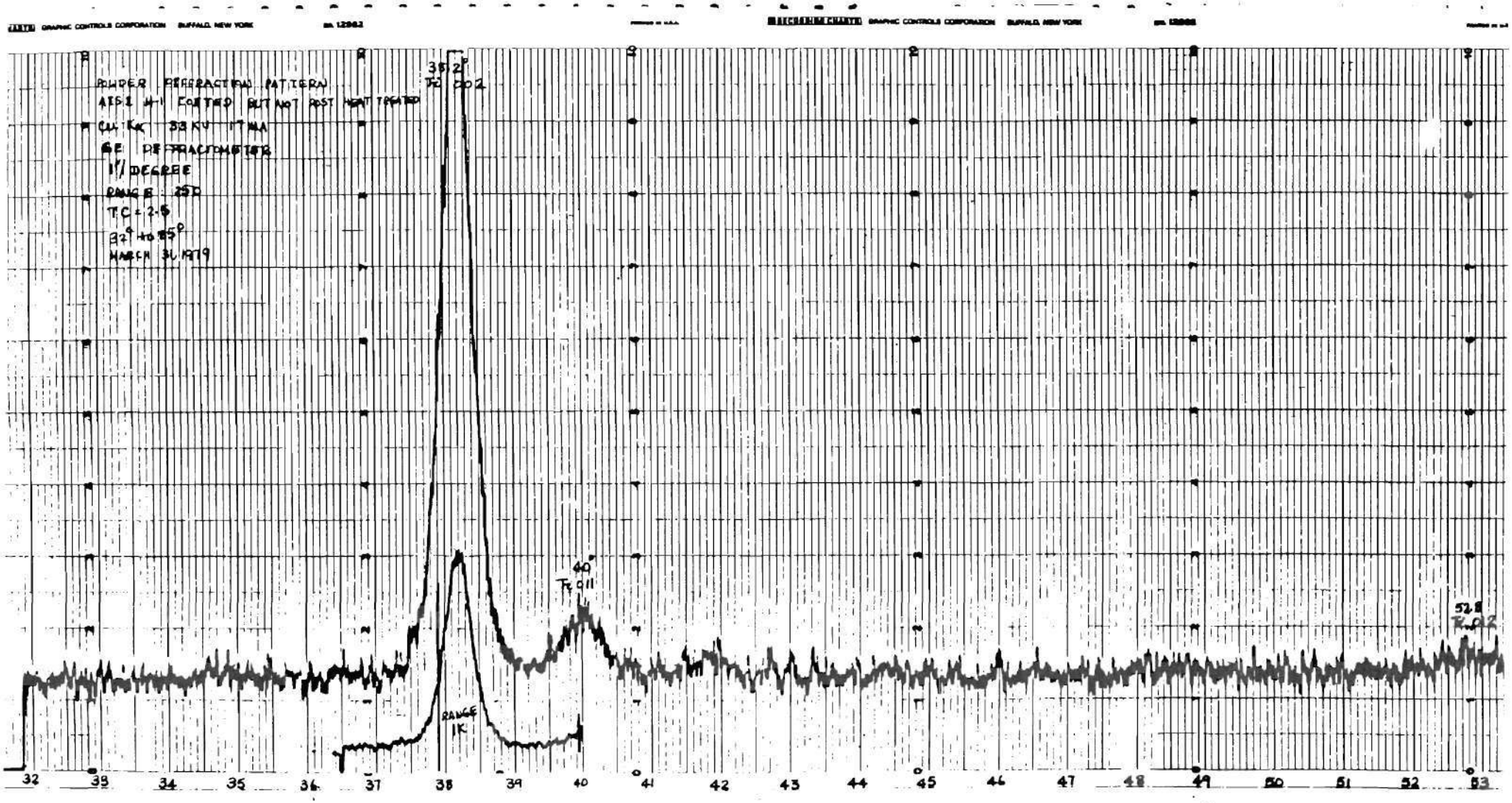

Figure B-1. Powder Diffraction (X-ray) Pattern of As-Coated AISI M-1 Tool

APPENDIX C

CALCULATION OF LATTICE PARAMETER OF COATED TiC[107]

TiC being a cubic crystal gives diffraction lines whose $\sin^2$ values satisfy the following equation, obtained by combining the Bragg law with the plane-spacing equation for the cubic system:

$$\frac{\mathrm{Sin}^2\theta}{(h^2 + k^2 + l^2)} = \frac{\lambda^2}{4a^2}$$

or

$$a^2 = \frac{\lambda^2}{4} \frac{1}{\left(\frac{\mathrm{Sin}^2\theta}{h^2+k^2+l^2}\right)}$$

For copper K_α radiation, $\lambda = 1.5420$ Å

$$\therefore \quad a^2 = \frac{0.5954}{\left(\frac{\mathrm{Sin}^2\theta}{h^2+k^2+l^2}\right)}$$

$$a = \sqrt{\frac{0.5954}{\left(\frac{\mathrm{Sin}^2\theta}{h^2+k^2+l^2}\right)}} \text{ Å}$$

The values of lines and the lattice parameter values are shown in Table C-1. Since the lattice parameter value is more accurate at high angles, the lattice parameter of the titanium carbide coating is obtained by extrapolating to high angles as shown in Figure C-1. The lattice parameter thus obtained for the coating in the present situation is 4.3784 Å. The lattice parameter value for $TiC_{1.0}$ is 4.3280 Å[33]. The above difference in lattice parameter probably is due to the presence of other elements such as oxygen in the coating.

Table C-1. Lattice Parameter of Coating

Line	θ	$\sin\theta$	$\sin^2\theta$	$h^2+k^2+l^2$	$\frac{\lambda^2}{4a^2}$	$a(\mathring{A})$
1	18.18	0.3119	0.0973	3	0.0324	4.2846
2	21.05	0.3592	0.1290	4	0.0323	4.2934
3	30.50	0.5075	0.2576	8	0.0322	4.3011
4	36.40	0.5934	0.3522	11	0.0320	4.3135

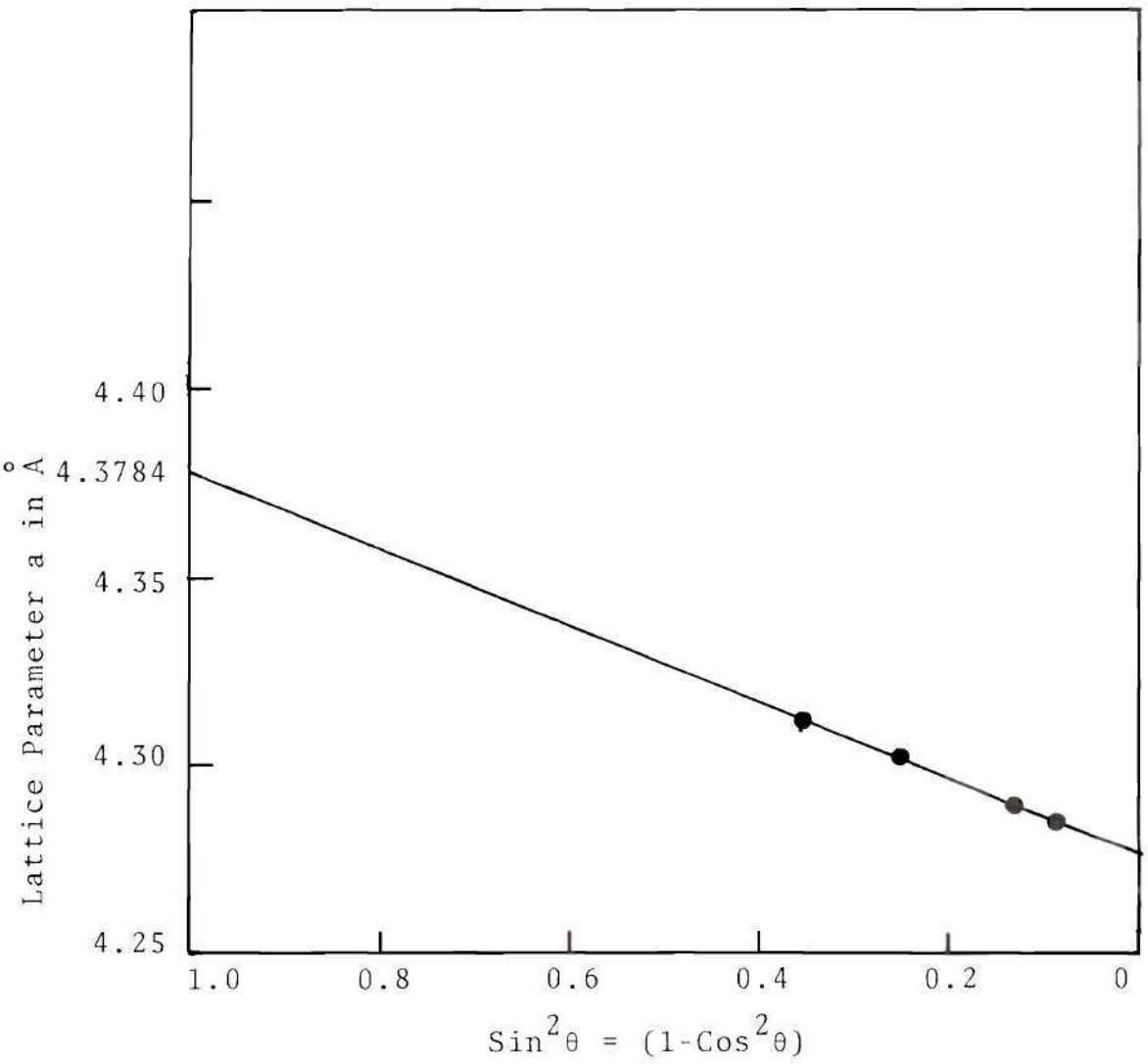

Figure C-1. Extrapolation Curve for Lattice Parameter of TiC Coating

APPENDIX D

MAGNETIC FIELD STRENGTH OF DC COIL

Magnetic field intensity H in amperes per meter generated by a coil of N turns is given by the following equation

$$H = \frac{NI}{2a}$$

where I is the current flowing through the coil and a is the radius of the circle formed by the coil, in meters.

Magnetic field strength B is given by $B = \mu H$ where μ is the permeability of the medium.

In the present case,

$a = 10 \text{ in} = .254 \text{ m}$

$I = 2.2$ amperes

$N = 608$

$$\therefore H = \frac{608(2.2)}{2(.254)} = 2633 \ \frac{\text{amperes}}{\text{meter}}$$

μ for air is given by $4\pi \times 10^{-7} \ \frac{\text{henry}}{\text{meter}}$

$$\therefore B = \mu H$$

$$= 4\pi \times 10^{-7} \frac{\text{henry}}{\text{meter}} \times 2633 \frac{\text{amperes}}{\text{meter}}$$

$$= 33088 \times 10^{-7} \frac{\text{henry amperes}}{\text{meter}^2} \text{ or } \frac{\text{weber}}{\text{m}^2}$$

$$= 33.088 \text{ Gauss } (\because 1 \text{ Gauss} = 10^{-4} \frac{\text{weber}}{\text{m}^2})$$

APPENDIX E

QUANTITATIVE AES ANALYSIS

Quantitative AES analysis is commonly performed using a semiempirical method which involves certain elemental sensitivity factors and assumes that differentiated Auger peak heights are proportional to the atomic concentrations. In spite of its limitation, accuracy of the order of 10% is possible.[108] The atomic concentration C_x can be expressed as

$$C_x = \frac{I_x}{S_x d_x}$$

where

I_x = Auger peak-to-peak amplitude

S_x = relative intensity

d_x = scale factor

The scale factor is the same for all peaks and therefore cancels out. The relative sensitivities for different elements involved at 3 keV are

$$S_C = 0.20$$

$$S_O = 0.50$$

$$S_{Ti} = 0.45$$

and

$$S_{Fe} = 0.20$$

The concentrations of different elements are calculated as follows:

$$C_C = \frac{\frac{I_C}{S_C}}{\frac{I_C}{S_C} + \frac{I_{Fe}}{S_{Fe}} + \frac{I_O}{S_O} + \frac{I_{Ti}}{S_{Ti}}}$$

The average peak to peak intensities and the calculated concentrations are shown in Table E-1.

Assuming all the carbon is associated with titanium C/Ti is calculated as $\frac{0.245}{0.280} = 0.875$. Therefore the stoichiometry of the titanium carbide as calculated from the Auger electron data is $TiC_{0.88}$. This value is slightly less than the value obtained by EPMA. $TiC_{0.93}$ at the center of the tool bit. Hence it is obvious that the stoichiometry obtained is not far from reality.

Table E-1. Atomic Concentration in the Coating

	C	Ti	O	Fe
I_x	733	1888	3454	422
I_x/S_x	3665	4196	6908	211
C_x	0.245	0.280	0.461	0.014

APPENDIX F

CALCULATION OF AMOUNTS OF TITANIUM AND CARBON IN THE COATING

AISI M-1 high speed steel contains 0.8% C. At 1200 C, the matrix contains about 0.44% carbon in solution and this is slightly greater than the equilibrium saturation value.[99] This assumes that vanadium, molybdenum and tungsten are satisfied with respect to their carbide (carbon) requirements. The number of atoms of carbon in austenite matrix and the number of atoms of titanium are calculated as follows.

Volume of HSS Tool = $(12.52)(12.52)(3.175)$

$= 497.68 \text{ mm}^3$

Density of HSS = $7.93 \frac{\text{gm}}{\text{cm}^3} = 7.93 \times 10^{-3} \frac{\text{gm}}{\text{mm}^3}$

Weight of HSS Tool = $(497.68)(7.93 \times 10^{-3})$

$= 3.947$ gm

Carbon available in austenite in 3.947 gm of HSS = $(\frac{0.44 \times 3.947}{100}) = .0174$ gm

Number of carbon atoms in austenite in HSS Tool = $(\frac{.0174}{12.01})(6.02 \times 10^{23})$

$= 8.72 \times 10^{23}$ atoms/tool

Volume of Titanium layer = $(12.52 \times 12.52 \times 2 \times 10^{-3})$

$= 0.3135 \text{ mm}^3$

Density of Titanium = $4.54 \frac{gm}{cm^3} = 4.54 \times 10^{-3} \frac{gm}{mm^3}$

Weight of 2 μm thick Ti layer = $(0.3135)(4.54 \times 10^{-3})$

$= 1.423 \times 10^{-3}$ gm

Number of titanium atoms in 2 μm thick layer = $(\frac{1.423 \times 10^{-3}}{47.9})(6.02 \times 10^{23})$

$= .179 \times 10^{20}$ atoms

$$\frac{\text{Atoms in 2 μm titanium}}{\text{Carbon atoms in austenite in HSS tool}} = \frac{.179 \times 10^{20}}{8.72 \times 10^{20}} \simeq \frac{1}{49}$$

APPENDIX G

USE OF EPMA FOR THIN FILM CHARACTERIZATION

Electron probe micro analyzer was used to analyze the chemistry of the coating on high speed steel tool inserts. This analysis was performed by Mr. James Johnson[114] and a statement given by him regarding the analysis is quoted below.

> The electron microprobe was used to analyze your samples of titanium carbide. In these analyses, the accelerating voltage used was selected so that the beam would not penetrate all of the TiC coating.
>
> It was determined that the above penetration did not occur by counting for iron, since the substrate was steel. No iron was found.

Therefore, it is justified to use EPMA for the chemical analysis of the coating on high speed steel in the present research.

APPENDIX H

TOOL-CHIP FRICTION COEFFICIENT CALCULATION

In order to verify the effect of coating (TiC) in reducing tool-chip coefficient of friction, a small experiment was performed with coated and uncoated tools. Cutting experiment performed was approximately orthogonal. Cutting forces and chip thickness were measured. The cutting conditions were 150 ft/min cutting speed, 0.005 in/rev feed and 0.060 in depth of cut. Coolant was used in both the cases. The data obtained is given below after calculating the friction coefficient using Merchant's analysis.

As is observed from Table H-1, the cutting forces as well as the friction coefficient (at the tool-chip interface) are less in case of coated tools when compared to uncoated tools. However the amount by which the cutting forces are reduced appears to be small. The coefficient of friction calculated using Amonton's laws in both cases appear to be the sticking type rather than sliding type.

Table H-1. Cutting Force and Friction Coefficient Data

		Uncoated Tool	Coated Tool
Main Cutting Force	lb	130	117
Thrust Force	lb	70	55
Chip Thickness	in	0.0167	0.0140
Friction Coefficient		0.66	0.58

APPENDIX I

SUBSTRATE-COATING INTERFACE HARDNESS

In order to investigate the hardness profile at the substrate-coating interface a taper sectioned specimen of the coated tool was prepared. The tool was first coated with a fiarly thick chromium support coating. The coated tool was then sectioned at about 45° using a Buehler Isomet low speed saw. The sectioned specimen was mounted, ground and polished. Micro-hardness measurements were taken on this taper sectioned specimen using Vickers Micro-Hardness Tester, Model 12a with 50 gms load. The data of the micro-hardness measurements is presented in Figure I-1 and a microphotograph indicating the indentations is presented in Figure I-2.

It appears that there is a hardness gradient over the substrate-coating interface which is to be expected because of diffusion bonding. There is a scatter in the micro-hardness of the coating (1963, 2467, 2823) which is within the range of micro-hardness data reported for titanium carbide (1500 VPN to 2800 VPN).[33]

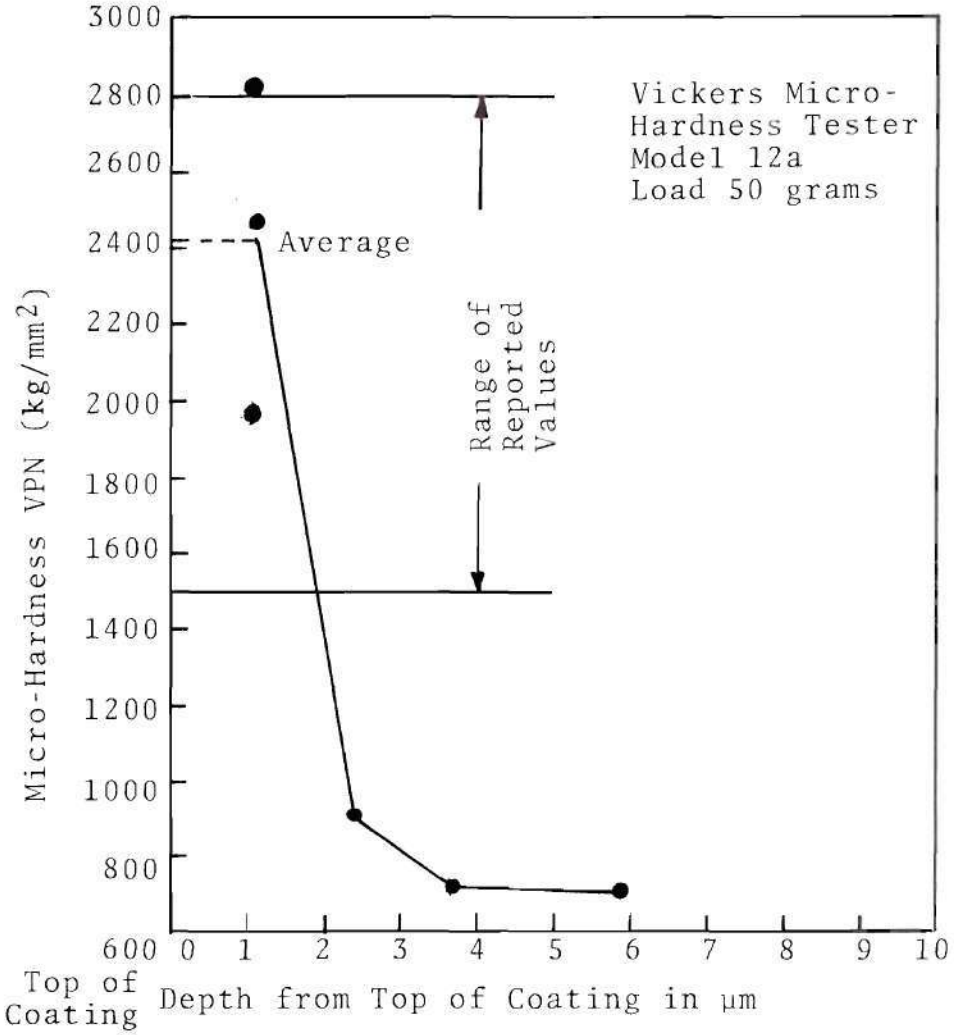

Figure I-1. Micro-Hardness Vs. Coating Depth

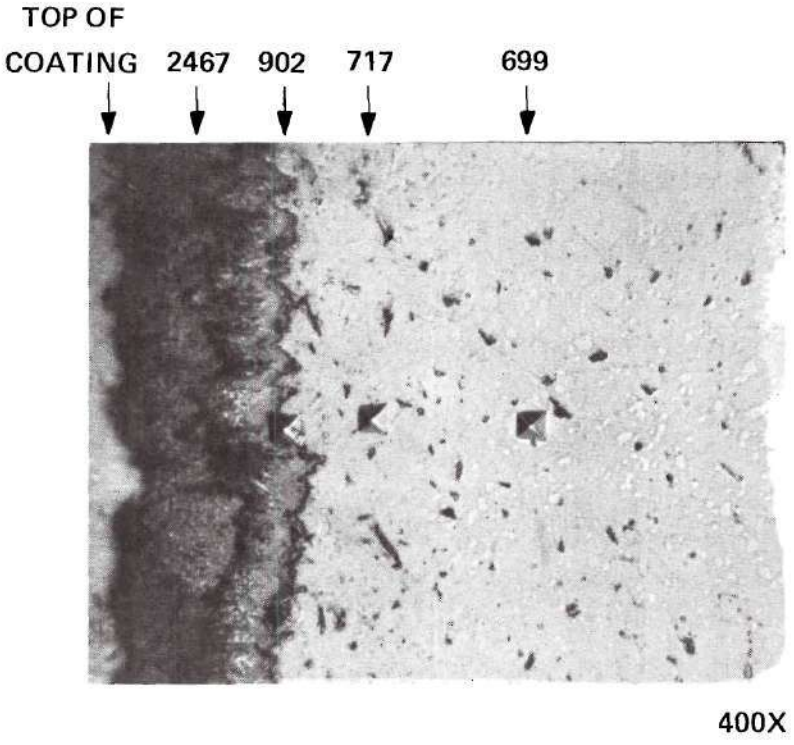

Figure I-2. Photomicrograph of Taper Section with Indentations

BIBLIOGRAPHY

1. C. Donaldson, G. H. LeCain and V. C. Goold: Tool Design. McGraw-Hill Book Company (New York) (1973).

2. Cornelius, A. M. Melis: Cutting Tool Material Selection. SME Technical Paper MR73-903.

3. SME: A Look at the Coatings...How Good are TiC, TiN, Hafnium and Aluminum Oxide. Manufacturing Engineering 78 (1977), No. 1 40/42.

4. J. T. Berry: High Performance High Hardness High Speed Steels. Climax Molybdenum Company (1970).

5. Kenneth P. Okley: Man the Tool Maker, British Museum.

6. M. E. Merchant, Hans Ernst and E. J. Krabacher: Radioactive Cutting Tools for Rapid Tool-Life Testing. Tr. ASME 75 (1953) 549/559.

7. K. J. Trigger and B. T. Chao: The Mechanism of Crater Wear of Cemented Carbide Tools. Tr. ASME 78 (1956) 1119/1126.

8. W. Dawihl: Influence of Diffusion and Alloy Formation on Resistance to Wear of Cemented Carbide Compositions. Zeitschrift Technische Physik 21 (1940) 44.

9. V. C. Venkatesh: Diffusion Wear of High-Speed Steels. Proc. 7th Inter. MTDR Conference (Birmingham) (1966) 401/413.

10. H. Opitz and W. Konig: On the Wear of Cutting Tools. Proc. 8th Inter. MTDR Conference (Manchester) (1967).

11. N. H. Cook: Tool Wear Tool Life. Tr. ASME 95 Series B (1973) No. 4 931.

12. P. K. Wright and E. M. Trent: Metallurgical Appraisal of Wear Mechanisms and Processes on High-Speed-Steel Cutting Tools. Metals Technology (1974) 13/23.

13. Norihoko Narutaki and Yasuo Yamane: Wear Mechanism of Carbide Tool Based on the Reaction Between Tool and Work Material (Part I Reaction Test). Bull. Japan Soc. of Precision Eng. 10 (1976) No. 3 95/100.

14. Norihoko Narutaki and Yasuo Yamane: Wear Mechanism of Carbide Tool Based on the Reaction Between Tool and Work Material (Part II Cutting Test and the Consideration of Tool Wear Mechanism). Bull. Japan Soc. of Precision Eng. 10 (1976) No. 4 133/138.

15. V. A. Zhilin and V. N. Tkachev: Role of Diffusion in the Wear of Carbide Cutting Tools. Fiz.-Khim. Mekh. Mat. 10 (1974) No. 4 80/83.

16. S. Ramalingam and Gloria Faulring: An Experimental Validation of the Abrasive Tool Wear Theory and the Conceptual Design of Ferrous Alloys for Machinability. Proc. Sixth NAMRC (Gainesville, Florida) (1978), 290/297.

17. J. D. Byrd and B. L. Ferguson: A Study of the Influence of Hard Inclusion on Carbide Tool Wear Utilizing a Powder Metal Technique. Proc. Sixth NAMRC (Gainesville, Florida) (1978) 310/316.

18. J. Hrbek: Sputtering of Metals in the Presence of Reactive Gases. Thin Solid Films 42 (1977) 185/191.

19. J. E. Greene and M. Pestes: Adhesion of Sputter-Deposited Carbide Films to Steel Substrates. Thin Films 37 (1976) 373/385.

20. K. Y. Su and N. H. Cook: Enhancement of High Speed Steel Tool Life by Titanium Nitride Sputter Coating. Proc. Fifth NAMRC (Massachusetts) (1977) 297/302.

21. D. M. Mattox: Film Deposition Using Accelerated Ions. Electrochemical Technology (Sept.-Oct. 1964) 295/298.

22. S. Aisenberg and R. W. Chabot: Physics of Ion Plating and Ion Beam Deposition. J. Vac. Sci. Technol. 10 (1973) No. 1 104/107.

23. R. F. Bunshah and A. H. Shabaik: Superhard Coatings for High-Speed-Steel Tools. Research/Development 26 (1975) No. 6 46/48.

24. R. F. Bunshah, A. H. Sahbaik, R. Nimmagadda and J. Covy: Machining Studies on Coated High Speed Steel Tools. Thin Solid Films 45 (1977) 453/462.

25. B. Zega, M. Kornmann and J. Amiguet: Hard Decorative TiN Coatings by Ion Plating. Thin Solid Films 45 (1977) 577/582.

26. R. J. Hill, G. Scheuermann and R. Lucariello: The Preparation of Hard Coatings Thin Solid Films 40 (1977) 217/222.

27. William R. Stowell: Ion-Plated Titanium Carbide Coatings. Thin Solid Films 22 (1974) 111/120.

28. Kazuo Nakamura and Konosuke Inagawa, Kazuyuki Tsuruoka and Souji Komiya: Applications of Wear Resistant Thick Films Formed by Physical Vapor Deposition Processes. Thin Solid Films 40 (1977) 155/167.

29. N. E. W. Hartley: The Tribology of Ion-Implanted Metal Surfaces. Tribology International (1975) 65/71.

30. J. T. Berry: Private Communication, 1978.

31. S. Ramalingam: Stoichiometry of TiC and Its Significance to the Performance of Hard Metal Compacts. Materials Science and Engineering 29 (1977) 123/130.

32. David Nicholls: Complexes and First-Row Transition Elements. American Elsevier Publishing Co. Inc. (1975).

33. Louis E. Toth: Transition Metal Carbides and Nitrides. Academic Press (New York) (1971).

34. Niels N. Engel and Eugene A. Anderson: U.S. Patent 3,988,955 (1976).

35. Thomas D. Harris: Improvement of Ion Plated Titanium and Titanium Carbide Coatings. MS Thesis submitted to the Faculty of the New Mexico Institute of Mining and Technology (1976).

36. Edmund Yung Chen: Effects of Ion Plating on Low Cycle Fatigue Behavior of Copper Single Crystals. Ph.D. Thesis Presented to the Faculty of the Division of Graduate Studies, Georgia Institute of Technology (1975).

37. G. Mah, C. W. Nordin and J. F. Fuller: Structure and Properties of Sputtered Titanium Carbide and Titanium Nitride Coatings. J. Vac. Sci. Technol., 11 (1974), No. 1 371/373.

38. W. W. Carson, N. H. Cook, B. M. Cramer, C. L. Leung and N. P. Suh: Annual Report NSF Hard Materials Research 3 (1974) 42.

39. W. D. Sproul and M. H. Richman: Reactive Sputtering of TiC with Oxygen. Thin Solid Films 28 (1975) L39/L40.

40. Airco Temescal: Physical Vapor Deposition. Airco. Inc. (Berkeley) (1976).

41. Eiji Tsunasawa, Kenichiro Inagaki and Kyuhiko Yamanta: Process Parameters and Some Properties of Ion-Plated Titanium Coatings on Steel Substrates, J. Vac. Sci. Technol., 14 (1974) No. 1.

42. M. Lee and M. H. Richman: Chemical Vapor Deposition of a TiC Coating a Cemented-Carbide Cutting Tool. Journal of the Electrochemical Society 120 (1973) No. 7 993/996.

43. K. G. Stjernberg, H. Gass and H. E. Hintermann: The Rate of Chemical Vapor Deposition of TiC. Thin Solid Films 40 (1977) 81/88.

44. H. O. Pierson: Titanium Carbonitrides Obtained by Chemical Vapor Deposition. Thin Solid Films 40 (1977) 41/47.

45. D. M. Mattox: Recent Advances in Ion Plating. Japan J. Appl. Phys. Suppl., 2 part 1 (1974) 443/449.

46. Peter J. Clarke: Magnetron DC Reactive Sputtering of Titanium Nitride and Indium-TiN Oxide. J. Vac. Sci. Technol. 14 (1977) No. 1 114/146.

47. S. Schiller, U. Heisig and K. Goedicke: On the Use of Ring Gap Discharges for High-Rate Vacuum Coating. J. Vac. Sci. Technol. 14 (1977) No. 3 815/818.

48. Mitsunori Kobayashi and Yoshihiko Doi: TiN and TiC Coating on Cemented Carbides by Ion Plating. Thin Solid Films 54 (1978) 67/74.

49. A. C. Raghuram and R. F. Bunshah: The Effect of Substrate Temperature on the Structure of Titanium Carbide Deposited by Activative Reactive Evaporation. J. Vac. Sci. Technol. 9 (1972) No. 6 1389/1394.

50. A. W. Czanderna: Methods of Surface Analysis. Elsevier Scientific Publishing Company (New York) (1975).

51. A. Wheeler: Structure and Properties of Solid Surfaces, edited by R. Gomer and C. S. Smith, University of Chicago Press (Chicago, Ill.) (1953) 455.

52. W. L. Latimer: Oxidation Potentials. Prentice-Hall, Inc., Englewood Cliffs (New Jersey), 1952.

53. G. Dearnaley and N. E. W. Hartley: Ion Implantation of Metals and Carbides. Thin Solid Films 54 (1978) No. 2 215/232.

54. M. Kodama, A. H. Shabaik and R. F. Bunshah: Machining Evaluation of Cemented Carbide Tools Coated with HfN and TiC by the Activated Reactive Evaporation Process. Thin Solid Films 54 (1978) No. 3 353/357.

55. R. F. Bunshah et al.: Structure and Properties of Refractory Compounds Deposited by Electron Beam Evaporation. Thin Solid Films 54 (1978) No. 1 85/106.

56. J. L. Peytary, A. Lebugle and G. Montel: A Study of Some Properties of Titanium Boronitride Used for the Coating of Cutting Tools. Wear 52 (1979) No. 1 89/94 paper presented at the 9th Plansee Seminar, Reulte, Austria, May 23-26, 1977.

57. Geoffrey Boothroyd: Fundamentals of Metal Machining and Machine Tools. Scripta Book Company (Washington, D.C.) (1975).

58. E. M. Trent: Metal Cutting. Butterworths (London, England) (1977).

59. Neil W. Sollenberger: Performance and Evaluation of Titanium Nitride Coatings. MS Thesis presented to the Faculty of the Division of Graduate Studies, Georgia Institute of Technology (1978).

60. M. A. Krishtal and U. F. Kozlov: Ti-Fe and Ti-Fe-C Interdiffusion. Izv. Uysslv. Uchebn, Zaved., Chern. Metall. 1977 (4) 76/81.

61. D. G. Teer: Adhesion of Ion Plated Films and Energies of Deposition. J. Adhesion 8 (1977) 289/300.

62. D. G. Teer et al.: The Role of Neutral Atoms in Ion Plating. J. Adhesion 8 (1976) 171/178.

63. N. K. Sharma and W. S. Williams: An Auger Analysis of Substrate Layer Interactions in the Chemical Vapor Deposition and Activated Reactive Evaporation of TiC. Thin Solid Films 54 (1978) 75/83.

64. N. Gane: New Types of Cutting Tool. Journal of Australian Institute of Metals. 21 (1976), No. 1 24/31.

65. R. F. Bunshah: High-Rate Evaporation Deposition Processes of Metals, Alloys, and Ceramics for Vacuum Metallurgical Applications, J. Vac. Sci. Technol., 11 (1974) No. 4 814/819.

66. D. G. Teer and F. B. Salem: The Formation of Low Friction Wear-Resistant Surfaces on Titanium by Ion Plating. Thin Solid Films 45 (1977) 583/589.

67. K. K. Yee: Protective Coatings for Metals by Chemical Vapor Deposition. International Metals Reviews (1978) No. 1 19/42.

68. W. A. Brainard and D. R. Wheeler: Use of a Nitrogen-Argon Plasma to Improve Adherence of Sputtered Titanium Carbide Coatings on Steel, J. Vac. Sci. Technol. 16 (1979), No. 1 31/36.

69. T. W. Hickmott and J. E. Baglin: Stoichiometry and Atomic Defects in RF-Sputtered SiO_2. J. Appl. Phys. 50 (1979) No. 1, 317/323.

70. N. A. Alford et al.: Auger Electron Spectrascopy (AES) An Appraisal. Surface and Interface Analysis I (1979) No. 1 36/44.

71. Nobuyuki Tamari and Akio Kato: Catalytic Effects of Various Metals and Refractory Oxides on the Growth of TiC Whiskers by Chemical Vapor Deposition. Journal of Crystal Growth 46 (1979) No. 2 221/237.

72. E. Lenz, D. Pnueli and L. Rozeanu: The Effect of a Thin Coating of Insulating Material on the Performance of Cutting Tools. Wear 53 (1979) 337/344.

73. M. Lee and M. H. Richman: Some Properties of TiC-Coated Cemented Tungsten Carbides. Metals Technology (1974) 538/546.

74. M. Lee, M. H. Richman and J. Stanislao: The Effect of a Coated Thin Surface Layer on the Wear of Cemented Carbide Tools. SME Paper FC71-929 1/18.

75. D. M. Mattox: Recent Advances in Ion Plating Japan J. Appl. Phys. Suppl. 2 pt. 1 1974 443/449.

76. L. C. Wu, J. L. Zilko, J. L. Mukherjee, J. E. Green and H. E. Cook: Tribology, Chemistry and Structure of Bias Sputtered TiC Films on Steel Substrates. International Conference on Wear, St. Louis, Missouri, 1977, 364/371.

77. V. K. Sarin, R. F. Bunshah and R. Nimmagadda: Structure of TiC-Ni Coatings Synthesized by Activated Reactive Evaporation. Thin Solid Films 40 (1977) 183/188.

78. N. Narutaki, K. Munakata, H. Kubo and K. Fukae: Cutting Performance of Coated Carbide Tools. Bull. Japan Soc. of Prec. Engg. 11 (1977) No. 4 205/206.

79. E. Easer, R. E. Ogilvie and K. A. Taylor: Structural and Compositional Characterization of Sputter-Deposited WC + Co Films. J. Vac. Sci. Technol. 15 (1978) No. 2 396/400.

80. F. Shinoki and A. Itoh: Mechanism of RF Reactive Sputtering. Journal of Applied Physics. 46 (1975) No. 8 3381/3384.

81. J. L. Mukherjee, L. C. Wu, J. E. Greene and H. E. Cook: Influence of Ar Sputtering Pressure on the Adhesion of TiC Films to Steel Substrates J. Vac. Sci. Technol. 12 (1975) No. 4 850/853.

82. S. K. Naik and N. P. Suh: The Formation of Oxycarbides During the Oxide Treatment of Cemented Carbide Tools. Paper presented at the Winter Annual Meeting, Nov. 19, detroit, Michigan, Paper No. 73-WA/Prod-16.

83. F. W. Taylor: On the Art of Cutting Metals. Trans. ASME 28 (1907) 331/350.

84. G. E. P. Box and K. J. Wilson: On the Experimental Attainment of Optimum Conditions. J. Roy Statist. Soc. Ser. B. 13 (1951) 1/45.

85. S. M. Wu: Tool Life Testing by Response Surface Methodology Part I, II. Trans. ASME Series B 86 (1964) 105/116.

86. R. Vilenchich, K. Strobele and R. Venter: Tool Life Testing by Response Surface Methodology Coupled with a Random Strategy Approach. Proceedings International Machine Tool Design and Research Conference (1968) 261/266.

87. S. K. Taraman and B. K. Lambert: Application of Response Surface Methodology to the Selection of Machining Variables. AIIE Transactions 4 (1972) No. 4 111/115.

88. P. C. Subbarao and C. H. Jacobs: Application of Nonlinear Goal Programming to Machining Variable Optimization. Paper presented at Sixth North American Metalworking Research Conference, Gainesville, Florida, 1978.

89. R. A. Williams and C. A. McGilchrist: Experimental Study of Drill Life. International Journal of Production Research, 10 (1972), No. 2 175/191.

90. Edward M. Mielnik: The Use of Fundamental Statistical Techniques in the Design of a Drilling Experiment. SME Paper MR73-163, 1973.

91. S. Ramalingam and J. D. Watson: Tool Life Distributions Part 1: Single-Injury Tool-Life Model. Transactions of ASME Ser B (1977).

92. S. Ramalingam: Tool Life Distributions Part 2: Multiple Injury Tool Life Model, Trans. ASME Ser. B (1977).

93. E. D. Doyle and L. E. Samuels: Metal cutting from a Materials Viewpoint. Journal of the Australian Institute of Metals 21 (1976), No. 1 2/15.

94. E. D. Doyle: Effect of Different Heat Treatments on the Wear of High Speed Steel Cutting Tools. Wear 27 (1974) 295/301.

95. O. L. Davies (Ed): The Design and Analysis of Industrial Experiments (1963) Oliver and Boyd, Edinburgh.

96. R. E. Devor, D. L. Anderson and W. J. Zdelblick: Tool Life Variation and Its Influence on the Development of Tool Life Models. Transactions of ASME Series B (1977).

97. Harold E. McGannon: The Making, Shaping and Treating of Steel, United States Steel (1971).

98. G. V. Samsonov and A. P. Epik: Coatings of High-Temperature Materials. Part I Edited by Henry H. Hausner Plenum Press, New York (1966).

99. Robert M. Brick, Alan W. Pense and Robert B. Gordon: Structure and Properties of Engineering Materials, McGraw-Hill Book Company, New York (1977).

100. John L. Vossen and Werner Kern: Thin Film Processes, Academic Press, New York (1978).

101. Ray E. Boltz and George L. Tuve (Ed.): CRC Handbook of Tables for Applied Engineering Science. CRC Press, Inc. 1976.

102. G. Dearnaley, J. H. Freeman, R. S. Nelson and J. Stephen: Ion Implantation, North-Holland Publishing Company (1973).

103. J. J. Gilman and B. W. Roberts: Elastic Constants of TiC and TiB_2. Journal of Applied Physics 32 (1961) 1405.

104. C. D. Turk and H. L. Marcus: The Mechanical Properties of Physical Vapor Deposited Titanium Transactions of the Metallurgical Society of AIME 242 (1968) 2251/2256.

105. R. F. Bunshah: Physical Vapor Deposition of Metals, Alloys and Ceramics, The 1974 Materials Science Symposium, New Trends in Materials Processing, American Society for Metals (1976) 200/269.

106. J. J. Cuomo, P. A. Leary, D. Yu, W. Reuter and M. Frisch: Reactive Sputtering of Carbon and Carbide Targets in Nitrogen. J. Vac. Sci. Technol. 16 (1979), No. 2 299/302.

107. B. D. Cullity: Elements of X-ray Diffraction, Addison-Wesley Publishing Company, Inc., Reading, Massachusetts (1967).

108. K. Fujimara, M. Ohtani, K. Kanayama and H. Ogata: Surface Science 61 (1976) 435.

109. M. C. Shaw and S. O. Dirke: On the Wear of Cutting Tools, Microtecnic 10 (1956) 187.

110. S. J. Deutsch and S. M. Wu: Analysis of Mechanical Wear During Grinding by Empirical Stochastic Models. Wear 29 (1974) 247/257.

111. S. Ramalingam, Y. I. Peng and J. D. Watson: Tool Life Distributions. Part 3 Mechanism of Single Injury Tool Failure and Tool Life Distribution in Interrupted Cutting. Journal of Engineering for Industry, Trans. ASME, Series B 100 (1978) No. 2 193/199.

112. S. Ramalingam and J. D. Watson: Tool Life Distributions Part 4. Minor Phases in Work Material and Multiple-Injury Tool Failure. Journal of Engineering for Industry, Trans. ASME, Series B 100 (1978) No. 2 201/209.

113. David R. Gaskell: Introduction to Metallurgical Thermodynamics (1973), Scripta Publishing Company, Washington.

114. James Johnson: Private Communication.

VITA

Potru China Subbarao, the only son of Mrs. and the late Mr. Potru Sree Ramulu, was born in Kollavaripalem, Andhra Pradesh, India, on September 22, 1948. He graduated from Regional Engineering College, Warangal, India in 1972 with a Bachelor of Engineering degree in Mechanical Engineering. He received a Master of Technology degree in Mechanical Engineering in 1974 from Indian Institute of Technology, Madras, India.

He has been a graduate student in the School of Mechanical Engineering at Georgia Institute of Technology since 1974.

He married the former Ghanta Parvati Devi on August 9, 1974. He is currently employed at Micromeritics Instrument Corporation in Norcross, Georgia.